

We are IntechOpen, the world's leading publisher of Open Access books Built by scientists, for scientists

6,900

Open access books available

186,000

International authors and editors

200M

Downloads

Our authors are among the

154

Countries delivered to

TOP 1%

most cited scientists

12.2%

Contributors from top 500 universities



WEB OF SCIENCE™

Selection of our books indexed in the Book Citation Index
in Web of Science™ Core Collection (BKCI)

Interested in publishing with us?
Contact book.department@intechopen.com

Numbers displayed above are based on latest data collected.
For more information visit www.intechopen.com



Roughness Effects on Turbulence Characteristics in an Open Channel Flow

Abdullah Faruque

Abstract

A comprehensive study was carried out to understand the effects of roughness on the turbulence characteristics of flow in an open channel and would be presented in this chapter. Tests were conducted with four different types of bed surface conditions (an impermeable smooth bed, impermeable rough bed, permeable sand bed and an impermeable bed with distributed roughness) and at two different Reynolds number ($Re = 47,500$ and $31,000$). The variables of interest include the mean velocity, turbulence intensity, Reynolds shear stress, shear stress correlation and higher-order moments. Quadrant decomposition was also used to extract the magnitude of the Reynolds shear stress from the turbulent bursting events. The effect of bed roughness on the turbulence characteristics can be seen throughout the depth of flow and thus dispute the 'wall similarity hypothesis'. In comparison to other roughness, distributed roughness shows the greatest effect on both streamwise and vertical turbulence intensities. Velocity triple products that reflects the transportation of turbulent kinetic energy is also seen to be affected by roughness of the channel bed with a variation of 200–300% compared to the flow over smooth bed. To analyze the turbulent bursting events, quadrant decomposition tools were used and found that the roughness affected heavily in the production of extreme turbulent events. The increases of the intensity and frequency of this turbulent burst causes the increase of instantaneous Reynolds shear stress. Transport of the sediment, pollutant suspension from the channel bed, changing the composition of the nutrient in the flow, sustainability of the benthic organisms, entrainment and exchange of energy and momentum are all influenced by this change of Reynolds shear stress. The sand used to form the various bed roughness conditions is same but found that the effect on different turbulence characteristics are different for different roughness. This is a strong indication that the geometric formation of the roughness is the cause of the differences in turbulence characteristics for different roughness formed by the same sand grain.

Keywords: turbulence, open channel flow, roughness, Reynolds shear stress, quadrant analysis, higher-order moment

1. Introduction

1.1 Open channel flow: general

Open channel flow comprises a sheared boundary layer like flow [1]. It is in utmost interest for the engineers and researchers to understand the structure and

dynamics of the open channel flow. Numerical modeling and laboratory experiments are two tools used by the researchers to explain the sediment transport, resuspension, formation of channel bed, entrainment in the flow and the exchange of energy and momentum in an open channel flow. Turbulence affects the horizontal and vertical transfer of energy and momentum and causes disruption to nutrition/oxygen utilization rates of some benthic organisms. Turbulent mixing increases with the increment of current speed and enhances the transport of phytoplankton. There were lot of studies with the explanation of mechanism of the above-mentioned phenomena but there are still a lot of unanswered questions and dispute. As indicated by [2] that a significant modulation of turbulence can be the result of average bed particle volume fractions as low as 10^{-4} . The other contribution factors to the modulation of turbulence are the shape, size and arrangement of bed particles. The research in open channel turbulent flow is much less comparing the vast amount of research done on turbulent boundary layer and pipe flow. Although there are significance in engineering application for the flow over rough surfaces but research study on turbulent flow over smooth surfaces [3–9] in both form of experimental and numerical since 1970 superseded the research on flow over rough surfaces. As research grows on the flows over rough surfaces but remains to be the Achilles heel of turbulent research [10]. There are basic differences between the flow in open channel and boundary layer due to the presence of the free surface and channel aspect ratio in an open channel flow and always debatable among researchers to use turbulent boundary layer data for modeling open channel flow [11]. Formation and enhancement of secondary currents occur due to the presence of the free surface and the side walls of the open channel. Free surface also dampens the vertical velocity fluctuations.

1.2 Open channel flow: effect of roughness

The flow progression from a developing state to a fully developed condition was studied by [12]. They have observed that for the case of a section with fully developed flow and the aspect ratio $b/d \geq 3$, the boundary layer extends to the surface of the water. At the channel centerline and near free surface, the velocity profile does not dip even for channel aspect ratio as low as $b/d = 3$. As discussed earlier about the differences between the flow in open channel and turbulent boundary due to the existence of free surface, [13] observed similarity on the velocity field due to the effect of roughness in a zero-pressure gradient turbulent boundary layer. The formation of secondary currents in an open channel flow is related to the aspect ratio (width/depth ratio of flow, b/d) and [7] noted the velocity-dip phenomenon for $b/d < 5$ where the measurement of maximum velocity on the centerline of a flume are seen to be below the free surface. In Ref. [14] indicated that the streamwise mean velocity profiles follow the well-known logarithmic law for the smooth surface, and with an appropriate shift, for the rough surface. In Ref. [15] observed that wall roughness led to higher turbulence levels in the outer region of the boundary layer. In Ref. [13] noted that roughness enhances the levels of the turbulence intensities over most of the flow.

Particle motion near a solid boundary causing sediment deposition and entrainment is influenced by the coherent structures near the wall as noted by [16] in their study of the particle behavior in the turbulent boundary layer. The generation of high-speed regions by vortices in the viscous layer sweeping along the wall causes particles pushing out of the way [16]. In Ref. [17] reported that for locations above the roughness sublayer, the distributions of the second-order turbulent stresses are

similar to the smooth-wall distributions. In Ref. [13] noted that roughness enhances the levels of the Reynolds shear stress over most of the flow. The specific geometry of the roughness elements causes significant enhancement to the levels of the Reynolds stresses as stated by [18]. The enhancement to the levels of the Reynolds stresses does not contain near the bed only but progresses over most of the flow creating a stronger interaction between the regions of flow (inner and outer) than would be implied by the wall similarity hypothesis.

In case of the three-dimensional flow (when $b/d \leq 5$) [7] predicted a reversal of the sign of the Reynolds shear stress ($-\overline{uv}$) from positive to negative at the location closer to the free surface. Correlation coefficient of the Reynolds shear stress is defined as ($R = \frac{-\overline{uv}}{u \times v}$) and is an indicator of the degree of similarity of turbulence-uv. The turbulence intensity in streamwise direction (u) and normal to the bed (v) is used to non-dimensionalize the Reynolds shear stress ($-\overline{uv}$). The correlation coefficient of the Reynolds stress only required the turbulence in streamwise and normal to the bed direction and [7] emphasized that the correlation coefficient of the Reynolds stress is very important because the estimation of the friction velocity is not required. The variation of R as stated by [7] is that after monotonous increment with respect to y/d in the region closer to the bed ($y/d < 0.1$) decreases as one moves away from near bed to the free-surface region. R attains a near constant value in the range of 0.4–0.5 for the middle portion of the flow depth ($0.1 \leq y/d \leq 0.6$). Properties of the mean flow in an open channel and the bed roughness have no effect on the value of R as noted by [7] and called the distribution of R universal. For an open channel flow [19] noted that the value of Reynolds shear stress increases to a maximum at the location closer to the bed and decreases after that. The researchers [19] explained that for the flow over smooth wall, the above mentioned variation of Reynolds shear stress is the effect of viscosity, whereas for the flow over rough bed, the emerging mechanisms for momentum extraction in the existing roughness sublayer is responsible. They blamed the lower value of aspect ratio that created secondary currents for the contradiction in the characteristics of the Reynolds stress with respect to the Reynolds number variation.

In Ref. [17] reported that the relative contributions of sweep and ejection events within the sublayer showed that sweep events provide the dominant contribution to the Reynolds shear stress within this region. In Ref. [13] noted that triple correlations and turbulence diffusion were strongly modified by the surface roughness. In Ref. [18] noted that surface roughness significantly enhances the levels of the turbulence kinetic energy, and turbulence diffusion in a way that depends on the specific geometry of the roughness elements. In Ref. [8] showed that the wall condition affects the variation of the triple products and the effects are not restrained to the near wall but extended to the full depth of flow. Ejection events shown clear dominance over other events for the full depth of the flow as noted by [8] and they also noted significant variation of ejection events with respect to bed roughness. To compare the effect of rough wall with smooth wall on the magnitude of the extreme events, they did the quadrant decomposition of the instantaneous velocity and found much higher magnitude for the flow over rough bed compared to the smooth wall flow. This is an indication of the effect of roughness propagating into the full depth of flow and not constraint to the region closer to the bed. Quadrant analysis is also done by [11] to compare the turbulent structures of open channel flow with the same in boundary layer flow. They found that the turbulent structures are very similar if all turbulent events are included in the analysis but found very significant difference if only the extreme events are used in analysis.

2. Experimental setup

2.1 Open channel flume

A 9-m long open channel flume at the University of Windsor with a rectangular cross-section dimension of 1100 mm \times 920 mm is used to perform the experiment. **Figure 1** shows the schematic of the experimental setup with open channel flume. A square cross-section dimension of 1.2 m and depth of 3 m header tank is placed at the beginning of the flume. The depth of flow for this series of experiments are kept to 100 mm, eventually achieving the aspect ratio (width/depth ratio of flow, b/d) of 11. Choice of this aspect ratio is based on the expectation that the generation of the secondary current will be minimum and the flow can be a representation of two-dimensional flow [7]. Two centrifugal pumps of 15 horsepower capacity each are used to recirculate the water. Tempered transparent glass materials are used to build the sidewalls and bottom of the flume and will enable the LDA (laser Doppler anemometer) to measure the instantaneous velocity. There were many previous studies [20–21] confirmed the quality of the flow of this permanent facility. The flume has an adjustable slope mechanism at the bottom but was kept horizontal for this series of test. 720 and 450 GPM are the two constant flow rate used for the tests.

2.2 Test conditions to study the effect of roughness

One hydraulically smooth and three characteristically different rough surfaces are used in this study to capture and understand the open channel flow characteristics. **Figure 2a** shows the hydraulically smooth bed condition made up by a polished aluminum plate spanning full width of the flume. Sand composed of uniform particles with gradation characteristics as shown in **Table 1** is used to create the three different rough surfaces. Four different types of bed surface conditions were used in this study. **Figure 2b** shows the ‘distributed roughness’ rough surface, **Figure 2c** shows the ‘continuous roughness’ rough surface and **Figure 3** shows the ‘natural sand bed’ rough surface. A 18 mm wide sand strip is glued on top of the polished aluminum plate spanning full width of the flume alternate by a 19 mm wide smooth strip to generate the distributed roughness. The same sand grain is glued on top of the entire polished aluminum plate spanning full width of the flume to generate the continuous roughness. Natural sand bed condition is consist of 3.7 m long 200 mm thick uniform sand of the same characteristics

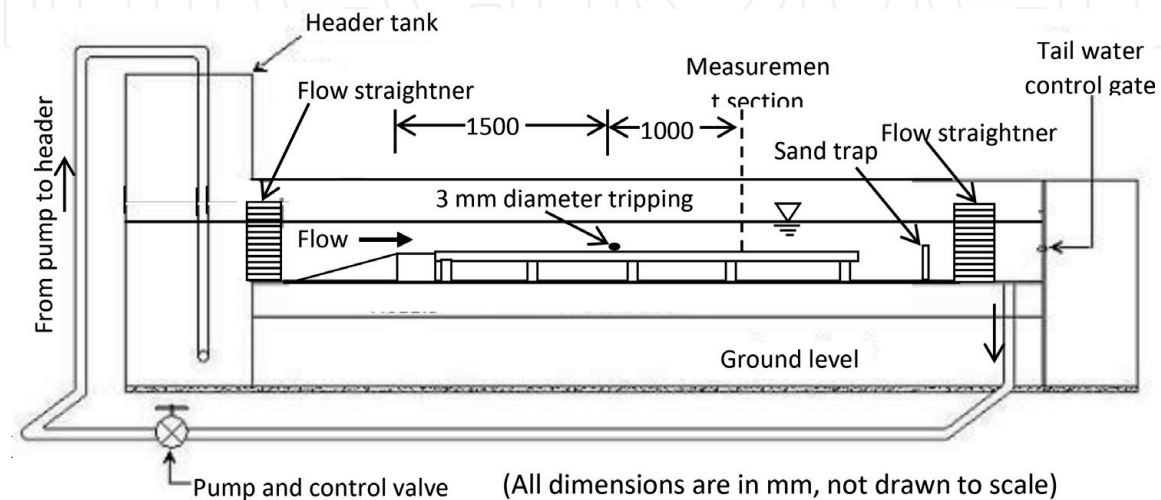


Figure 1.
Schematic of the open channel flume and experimental setup.

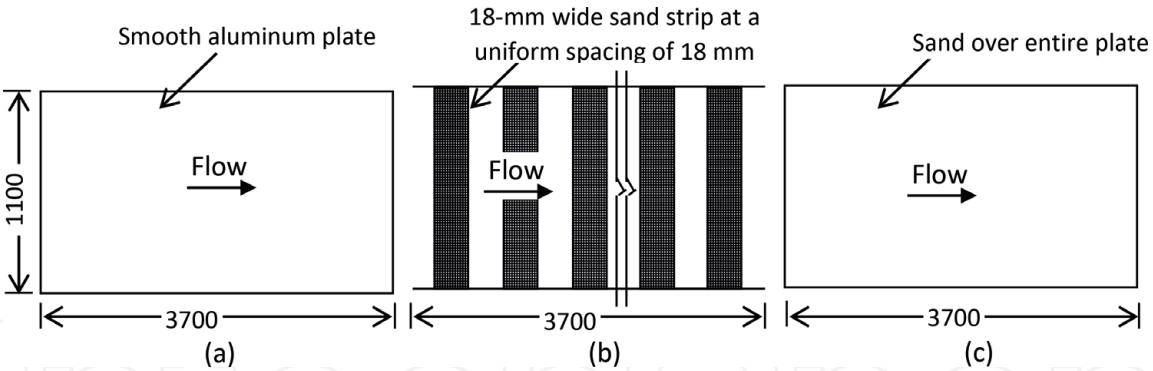


Figure 2. Plan view of different fixed bed condition. (a) Hydraulic smooth surface, (b) Distributed roughness surface, (c) Continuous roughness surface.

d_{50} (mm)	2.46
d_{95}/d_5	1.91
d_{95}/d_{50}	1.34
d_{84}/d_{50}	1.26
$\sigma_g = \sqrt{d_{84}/d_{16}}$	1.24
$C_z = d_{30}^2/(d_{60}d_{10})$	1.00

Table 1. Gradation measurements of the sand.

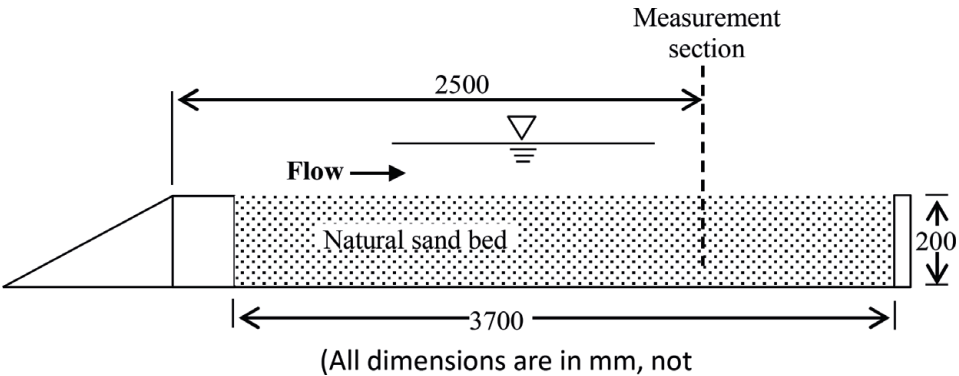


Figure 3. Section of natural sand bed.

spanning full width of the flume. Special care had been taken in maintaining the flow condition in such a way that there were no sand movement in any period of time of running the test. As a precautionary measure of accidental sand movement and sand entering into the pipe/pump system causing damage to the pump, a sand trap is constructed at the end of the flume.

Two different flow Reynolds numbers ($Re = U_{avg}d/\nu \approx 47,500$ and $31,000$) correspondence to two different Froude numbers ($Fr = U_{avg}/(gd)^{0.5} \approx 0.40$ and 0.24) respectively are used for each four bed surface conditions. The parameters used for Reynolds and Froude number calculations are the average streamwise velocity (U_{avg}), nominal depth of flow (d), kinematic viscosity of the fluid (ν) and gravitational acceleration g . The flow conditions are maintained to be subcritical (i.e., Froude numbers less than unity) and choose the flow Reynolds numbers accordingly. The variation of water surface elevation were measured for the test section and there are less than 1 mm variation of surface water for a streamwise distance of 600 mm proves that pressure gradient is negligible. In order of conditioning the flow, two sets of flow straighteners are placed at the beginning and end

of the flume. A turbulent boundary layer presence is ensured by tripping the flow using a 3 mm diameter rod at the upstream of the measurement section as shown in **Figure 1**. Shape factor of the boundary layer (the ratio of displacement to momentum thickness) for the flow over smooth bed is found for this case as 1.3 and flow can be considered as fully developed turbulent flow [22]. The instantaneous velocity measurement is carried out on top of the 60th sand strip for the flow over distributed roughness bed. To minimize the effect of secondary current, measurements for all flow test conditions are carried out along the flume centerline. Preliminary tests for all bed conditions are carried out to confirm that the flow condition is fully developed. **Table 2** presents the summary of various test conditions.

2.3 The laser Doppler anemometry

Velocity measurements were done using A commercial two-component fiber-optic LDA system (Dantec Inc.) which is powered by a 300-mW Argon-Ion laser. Details of this is avoided for brevity because using the same system in several previous studies [20, 23, 9]. A Bragg cell and a focusing lens of 500 mm with beam spacing of 38 mm are the optical elements of the LDA system. A large amount of data collected (10,000 validated samples at each and every measurement location) to minimize the uncertainty of the data collection. The data rate varied widely based on the location of the measurement and ranges from 4 Hz to 65 Hz. The water used in the test is seeded with hollow spheres with density of 1.13 g/cc with mean particle size of 12 microns after filtering the water for many days and it is done prior to the start of the measurement. The seeded particles can stuck on the flume side wall and can cause extraneous scattered light distributed throughout the illuminating beams. The glass side wall around the measurement region were cleaned before each set of measurement to avoid the erroneous data collection due to the scattered light. Due to the measurement location at the flume centerline, two scattered beams of the present two-component LDA system measuring the vertical component of the velocity cannot reach at very close to the bed or very close to the free surface but measurement of streamwise one-component velocity were carried out for full depth of flow. Following the footsteps of other researchers [16, 6] who have successfully tilted the probe by 3° and 2°, respectively, in their pursuit to collect two dimensional velocity data closer to the wall, the LDA probe for the present tests was tilted 2° towards the bottom wall to capture data for two-component velocity measurements at near proximity of the wall.

Test	Bed condition	d (mm)	Re	Fr
1	Smooth bed	~100	~47,500	~0.40
2		~100	~31,000	~0.24
3	Distributed roughness	~100	~47,500	~0.40
4		~100	~31,000	~0.24
5	Continuous roughness	~100	~47,500	~0.40
6		~100	~31,000	~0.24
7	Natural sand bed	~100	~47,500	~0.40
8		~100	~31,000	~0.24

Table 2.
Summary of test conditions to study the effect of roughness.

3. Results and discussions

The purpose of the present study is to explain how the roughness and Reynolds number affect flow characteristics in an open channel flow (OCF). Tests were conducted with four different types of bed surface conditions (an impermeable smooth bed, impermeable rough bed, permeable sand bed and an impermeable bed with distributed roughness) and at two different Reynolds number ($Re = 47,500$ and $31,000$) for each and every bed surface. Instantaneous velocity components are used to analyze the streamwise mean velocity, turbulence intensity in both streamwise and vertical direction, Reynolds shear stress including shear stress correlation and higher-order moments including vertical flux of the turbulent kinetic energy. Quadrant decomposition was also used to extract the magnitude of the Reynolds shear stress from the turbulent bursting events.

3.1 Mean velocity profiles

3.1.1 Outer coordinates

Figure 4 shows the variation of streamwise component of the velocity with respect to the depth of flow in outer coordinates. The mean velocity (U) is non-dimensionalize by the maximum velocity (U_e) and the wall normal distance (y) is non-dimensionalize by the maximum flow depth (d). As one can see in the inset in **Figure 4** that the velocity profiles of every flow conditions show a slight dip in the outer region where the location of maximum velocity happened to be occurred below the free surface with dU/dy is negative in the location close to the free surface. Velocity dip is different with different rough bed conditions with flow over natural sand bed showing the biggest dip followed by distributed roughness and continuous roughness bed. However, the flow over smooth surface shows the dip higher than the flow over distributed roughness and continuous roughness bed. Effect of bed roughness is very evident at the location close to the bed with velocity profile for the flow over smooth wall is fuller compared the flow over different rough beds. The same phenomenon was also observed by [15] and blamed it to the increment of surface drag due to the effect bed roughness. Comparing the effect of various type of bed roughness on the streamwise velocity component as one can see from **Figure 4a** that distributed roughness profile has the biggest deviation from smooth bed profile with continuous roughness and natural sand bed shows identical deviation. The variation of streamwise component of the velocity with respect to the depth of flow in outer coordinates with respect to the lower Reynolds number is shown in **Figure 4b**. The velocity profile characteristics are very similar for the lower Reynolds number flow compared to the flow for higher Reynolds number with the exception of flow over natural sand bed, which shows much higher deviation than flow over the bed of continuous roughness. One can correlate this with the interchange of fluid and momentum across the boundary, which is permeable like the flow over the bed of natural sand. The subsequent momentum/energy loss due to the effect of infiltration and corresponding differences on mean velocity reduces with the increment of Reynolds stress.

3.1.2 Inner coordinates

Figure 5 shows the variation of streamwise component of the velocity with respect to the depth of flow in inner coordinates. The Clauser method was used to calculate the friction velocity for flow over smooth and rough bed conditions by

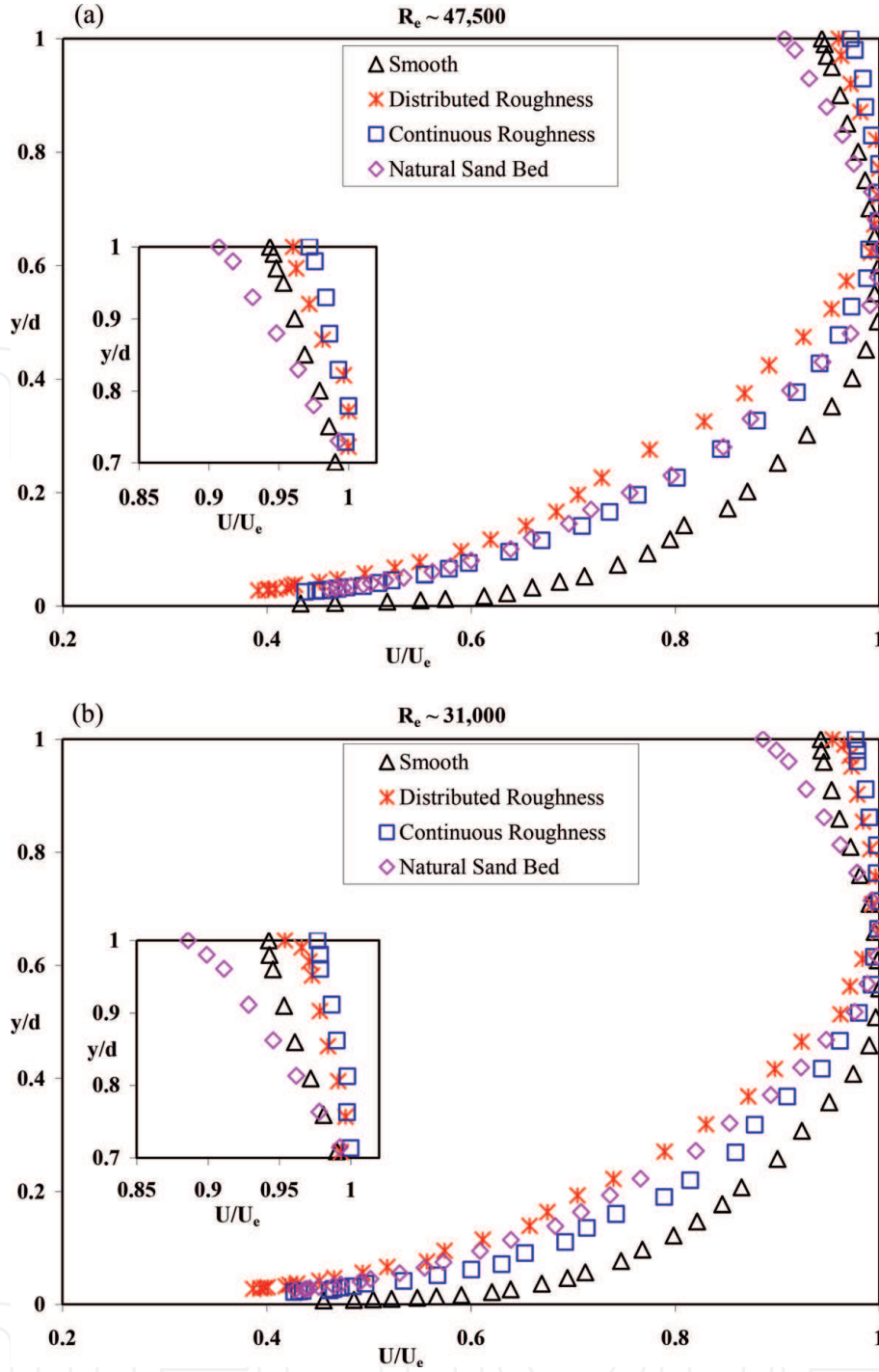


Figure 4.
Streamwise mean velocity profile for flow over different bed condition.

fitting the respective mean velocity profiles of different bed conditions with the classical log law, $U^+ = \kappa^{-1} \ln y^+ + B - \Delta U^+$. Log-law constants used here are $U^+ = U/U_\tau$, $y^+ = yU_\tau/\nu$, $\kappa = 0.41$, $B = 5$ and the downward shift of the velocity profile represented by the roughness function ΔU^+ with $\Delta U^+ = 0$ for the flow over the bed which is smooth. The present test data over the smooth bed has better agreement with the standard log-law represented by the solid line. For the flow over rough beds there are downward shift of the profile compared to the smooth bed which is fully expected and clearly visible. The effect of roughness can be measured by the downward shift of the profile and one can note from **Figure 5a** that the distributed roughness shows the highest deviation from the smooth bed with flow over natural sand bed shows the least deviation and flow over continuous roughness fall in-between. The variation of streamwise component of the velocity with respect to the

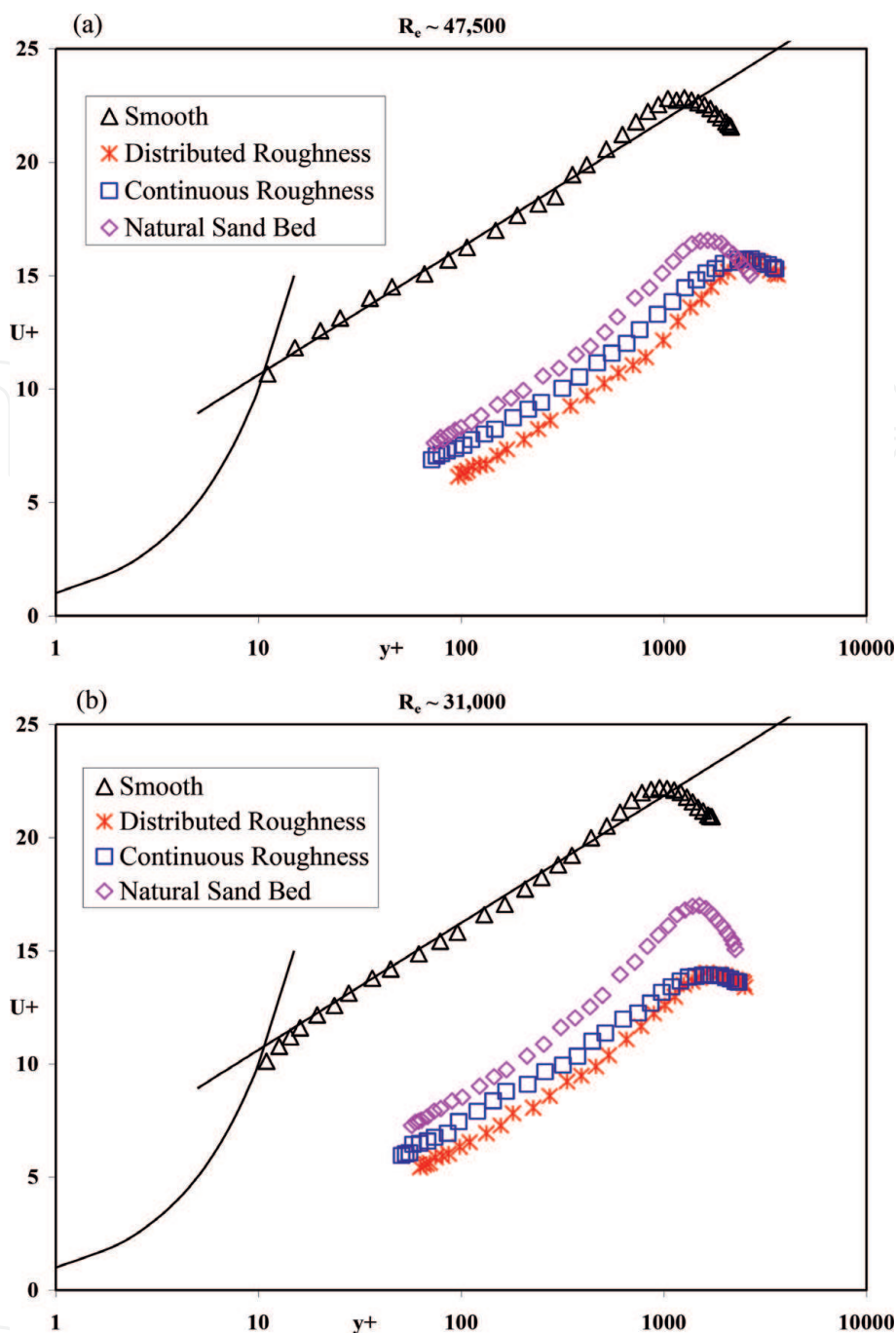


Figure 5.
Mean velocity profile in inner coordinates for flow over different bed condition.

depth of flow in inner coordinates with respect to the lower Reynolds number is shown in **Figure 5b**. The velocity profile characteristics are very similar for the lower Reynolds number flow compared to the flow for higher Reynolds number.

The magnitude of friction coefficient C_f ($C_f = 2(U_\tau/U_e)^2$) is found to be dependent on the type of bed roughness with distributed roughness has the highest value followed by the flow over the continuous roughness bed surface and the sand bed. The magnitude of friction coefficient is also found to be dependent on the Reynolds number with the reduction of the magnitude of friction coefficient with the increment of the Reynolds number. The magnitude of C_f is seen to be smaller for the flow over a permeable bed (natural sand bed) compared to the flow over an impermeable bed (distributed and continuous roughness bed). One can correlate this with the development of finite slip velocity across the permeable boundary layer causing the reduction of the magnitude of friction compared to the flow over impermeable layer. In contrary, [24] discovered that for the boundaries with similar rugosity the

magnitude of friction resistance is seen to be higher for the flow over a permeable bed compared to the flow over an impermeable bed. Dissipation of energy happened in the transition zone of the porous permeable medium with added loss of energy due to interchange of fluid and momentum across the permeable boundary translated back into the main flow. They commented that the net effect of combined energy loss might be responsible for the higher resistance.

3.2 Turbulence intensity

3.2.1 Streamwise turbulence intensity

The distribution of the streamwise component of the turbulence intensity for flow over both smooth and rough beds is shown in **Figure 6**. Computed quantities

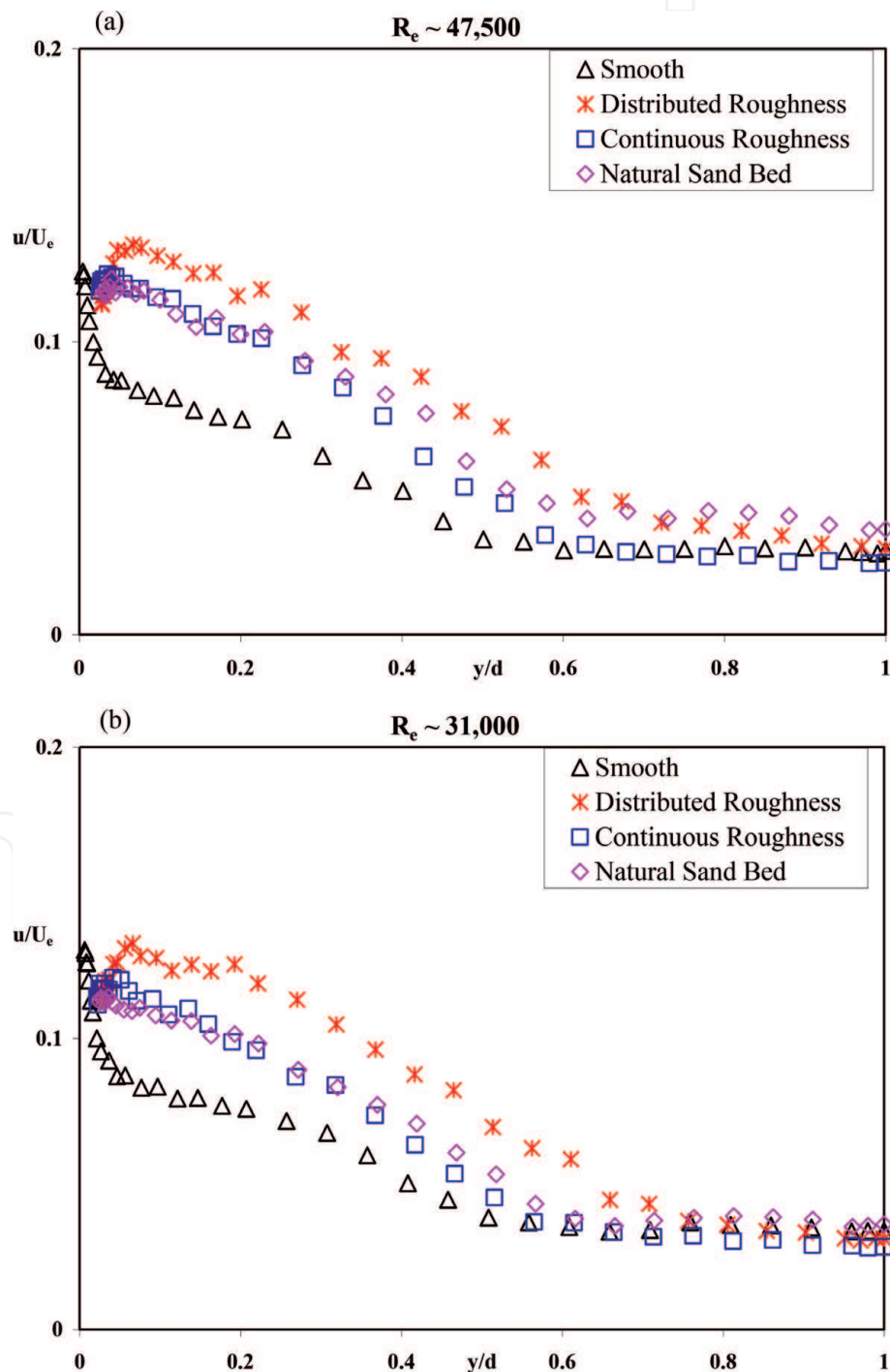


Figure 6.
Streamwise turbulence intensity for flow over different bed condition.

can bring additional uncertainties in relation to the scaling parameters and to avoid any additional uncertainties, the streamwise turbulent intensity (u) is non-dimensionalized by the maximum velocity (U_e) and the wall normal distance (y) is non-dimensionalized by the maximum flow depth (d). Magnitude of the streamwise component of the turbulence intensity reaches to the maximum at the location very close to the bed irrespective of the bed condition as one can note from **Figure 6a**. The location of maximum streamwise component of the turbulence intensity is different with different bed conditions. The location of the peak for the flow over smooth bed is very close to the bed at $y/d \sim 0$, whereas the peak for the flow over rough surfaces varies with the different type of roughness. As one can note from **Figure 6a** that the distributed roughness shows the highest peak compared to the flow over continuous roughness and flow over natural sand bed. The location of the peak for the flow over rough beds are also varied depending on the type of roughness. The location of the peak for the flow over distributed roughness is at around $y/d \sim 0.08$ whereas the location of the peak for the flow over continuous roughness and natural sand bed have occurred at the same location of $y/d \sim 0.04$ which is a distance closer to the bed compared to the flow over distributed roughness. Immediately after reaching the peak the streamwise component of the turbulence intensity for flow over both smooth and rough beds reduces but the trend of reduction is very different for the flow over smooth bed compared to the flow over rough surfaces. There is a sharp drop of the magnitude of the streamwise component of the turbulence intensity for the smooth bed before a more constant drop towards the free surface and reaching a near constant value at $y/d \sim 0.5$. For the flow over rough surfaces the drop of the value towards the free surface after the peak is linear and attains a near constant value but the location and magnitude of constant value is different for different rough surfaces (distributed roughness does not attain constant value but variation near free surface is minimal). The location of a near constant value for the flow over continuous roughness and natural sand bed is at the same level of $y/d \sim 0.62$. The streamwise component of the turbulence intensity near the free surface also shows the effect of roughness with natural sand bed shows the highest intensity followed by the distributed roughness with flow over continuous roughness is the lowest. The effect of roughness on the distribution of the streamwise component of the turbulence intensity is very evident throughout the flow depth with distributed roughness shows the highest deviation followed by natural sand bed and continuous roughness compared to the smooth surfaces with the exception at the location very close to the bed. Although the sand grain used to create all three bed roughness is of the same gradation characteristics but the geometry of the roughness formation is different causing the differences in the distribution of the streamwise component of the turbulence intensity.

The variation of streamwise component of the turbulence intensity with respect to the depth of flow for the flow conditions to the lower Reynolds number is shown in **Figure 6b**. The streamwise component of the turbulence intensity profile characteristics are very similar for the lower Reynolds number flow compared to the flow for higher Reynolds number with the exception of flow over distributed roughness bed, which shows much higher deviation than flow over the smooth bed at the lower Reynolds number. In lower Reynolds number flow, the differences in streamwise component of the turbulence intensity for continuous roughness and natural sand bed is negligible.

3.2.2 Vertical turbulence intensity

The distribution of the vertical component of the turbulence intensity for flow over both smooth and rough beds is shown in **Figure 7**. Significant effect of

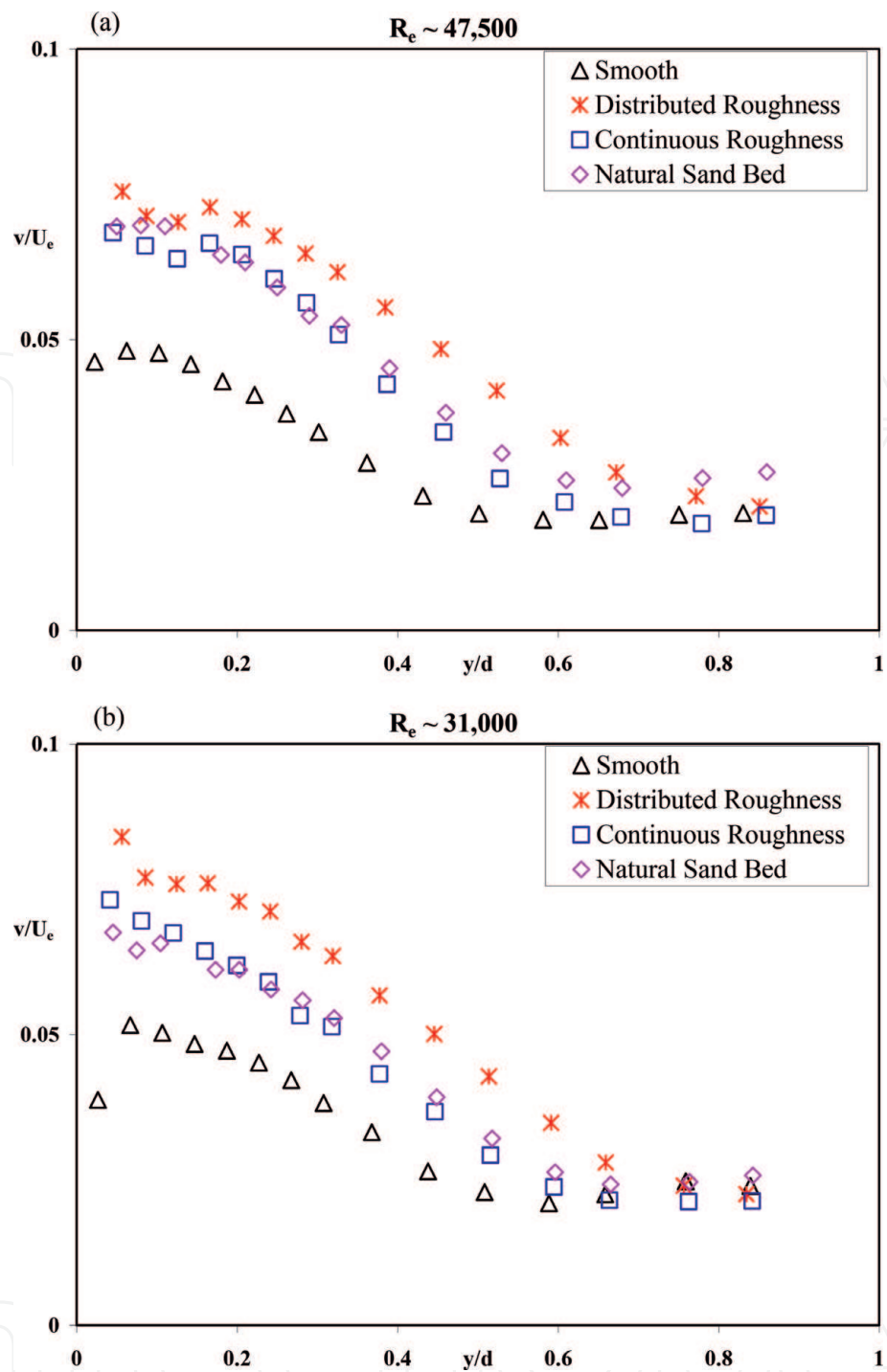


Figure 7.
Vertical turbulence intensity for flow over different bed condition.

roughness can be seen for lower two third of the depth of flow with the effect tapered off at the location closer to the surface. Comparing the effect of various type of bed roughness on the vertical component of the turbulence intensity as one can see from **Figure 7a** that distributed roughness profile has the biggest deviation from smooth bed profile with continuous roughness and natural sand bed shows identical deviation for most the depth of the flow. For the location closer to the surface, the flow over natural sand bed shows higher magnitude of the vertical component of the turbulence intensity compared to any other surfaces. The variation of the vertical component of the turbulence intensity for flow with respect to the lower Reynolds number is shown in **Figure 7b**. The profile characteristics are very similar for the lower Reynolds number flow compared to the flow for higher Reynolds

number with the exception that there are almost no effect of roughness on the vertical component of the turbulence intensity for the location closer to the surface.

3.3 Reynolds shear stress

The distribution of the Reynolds shear stress in outer variables for flow over both smooth and rough beds is shown in **Figure 8**. Magnitude of the Reynolds shear stress reaches to the maximum at the location very close to the bed ($y/d < 0.2$) irrespective of the bed condition as one can note from **Figure 8a**. Effect of roughness on the Reynolds shear stress is very evident for lower two third of the depth of flow with the effect tapered off at the location closer to the surface. The peak for the flow over rough surfaces varies with the different type of roughness. As one can

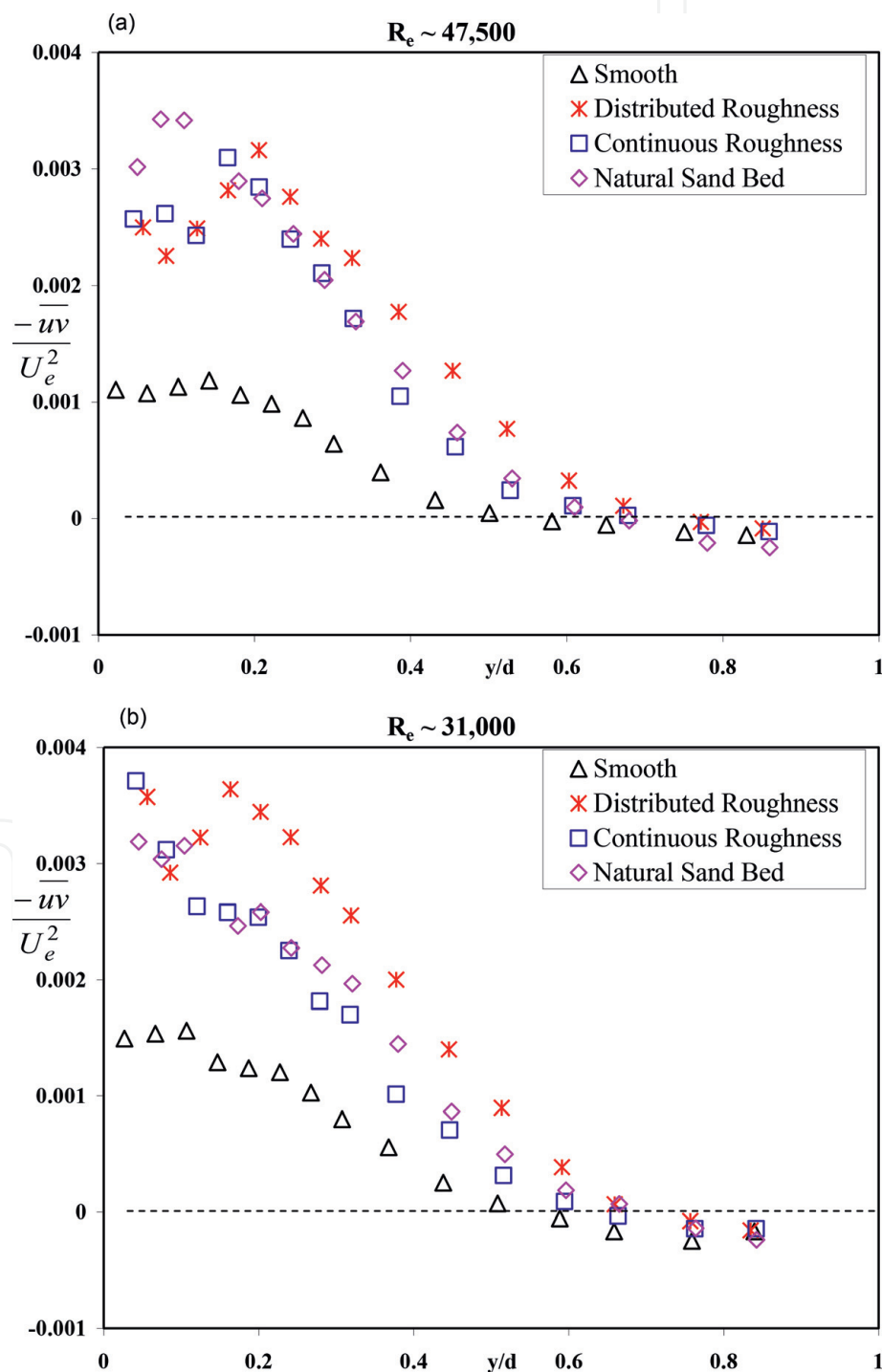


Figure 8.
Reynolds shear stress distribution for flow over different bed condition.

note from **Figure 8a** that the flow over natural sand bed shows the highest peak compared to the similar peak for flow over continuous roughness and flow over distributed roughness. Immediately after reaching the peak the Reynolds shear stress for flow over both smooth and rough beds reduces but the trend of reduction is very different for the flow over smooth bed compared to the flow over rough surfaces. There is a sharp drop of the magnitude of the Reynolds shear stress for the rough beds compared to the smooth bed before a more constant drop towards the free surface. For the region further away from the near bed ($y/d > 0.2$), flow over distributed roughness shows generation of higher Reynolds shear compared to the other two rough beds where the generation of the Reynolds shear stress is very similar. As one can see in **Figure 8a** that the Reynolds shear stress falls below zero and becomes negative in the location close to the free surface for flow over both smooth and rough beds. The location of zero Reynolds shear stress is different for flow over smooth bed (at $y/d \sim 0.5$) compared to the flow over rough beds ($y/d \sim 0.7$). The location of negative Reynolds shear stress for different bed conditions are on the same location where dU/dy is negative as one can see in **Figure 4**. Few other researchers [25, 6, 26] found the visible effect of roughness on Reynolds shear stress for the depth of flow $y/d \approx 0.2-0.3$ but the distinct effect of roughness for the present study can be seen penetrating deep into the flow $y/d \approx 0.7$. In case of the study by [3] where the researcher did not find any effect of roughness (2 mm sand and 9 mm pebbles) on Reynolds shear stress compared to the flow over smooth bed. The sample size used for the tests by [3] were rather very small rendered to the unexpected conclusion. The variation of the Reynolds shear stress for flow with respect to the lower Reynolds number is shown in **Figure 8b**. The profile characteristics are very similar for the lower Reynolds number flow compared to the flow for higher Reynolds number with one of the exception is that the flow over continuous roughness and flow over distributed roughness shows the similar highest peak compared to the flow over natural sand bed. Another exception can be seen as much higher generation of Reynolds shear stress for the flow over distributed roughness for the region further away from the near bed ($y/d > 0.2$) followed by flow over natural sand bed and continuous roughness.

3.4 Shear stress correlation coefficient

The distribution of the correlation coefficient of the Reynolds shear stress ($R = \frac{-\overline{uv}}{u \times v}$) for flow over both smooth and rough beds is shown in **Figure 9**. One can state that R is the expression of a normalized covariance where degree of similarity between the streamwise component of the turbulence intensity and the vertical component of the turbulence intensity is established. The range of the R as $-1 \leq R \leq 1$ where the value of $R = 1$ is the indication that the linear relationship between the streamwise component and the vertical component of the turbulence intensity is increasing. The value of $R = -1$ is the indication that the linear relationship between the streamwise component and the vertical component of the turbulence intensity is decreasing. Local statistics of R at a particular location can be an indication of the presence or absence of any flow structures. The effect of roughness on the variation of R is mixed compared to the smooth bed flow. As one can see from **Figure 9a** that at the location close to the bed ($y < 0.3d$) the magnitude of R is very similar for flow over smooth bed compared to the flow over distributed roughness with much higher value of R for the flow over continuous roughness and natural sand bed. The effect of roughness for the outer layer ($y > 0.3d$) is very clear with value of R is consistently higher for the flow over all three rough beds compared to the flow over smooth bed. One can also see from **Figure 9a** that the value

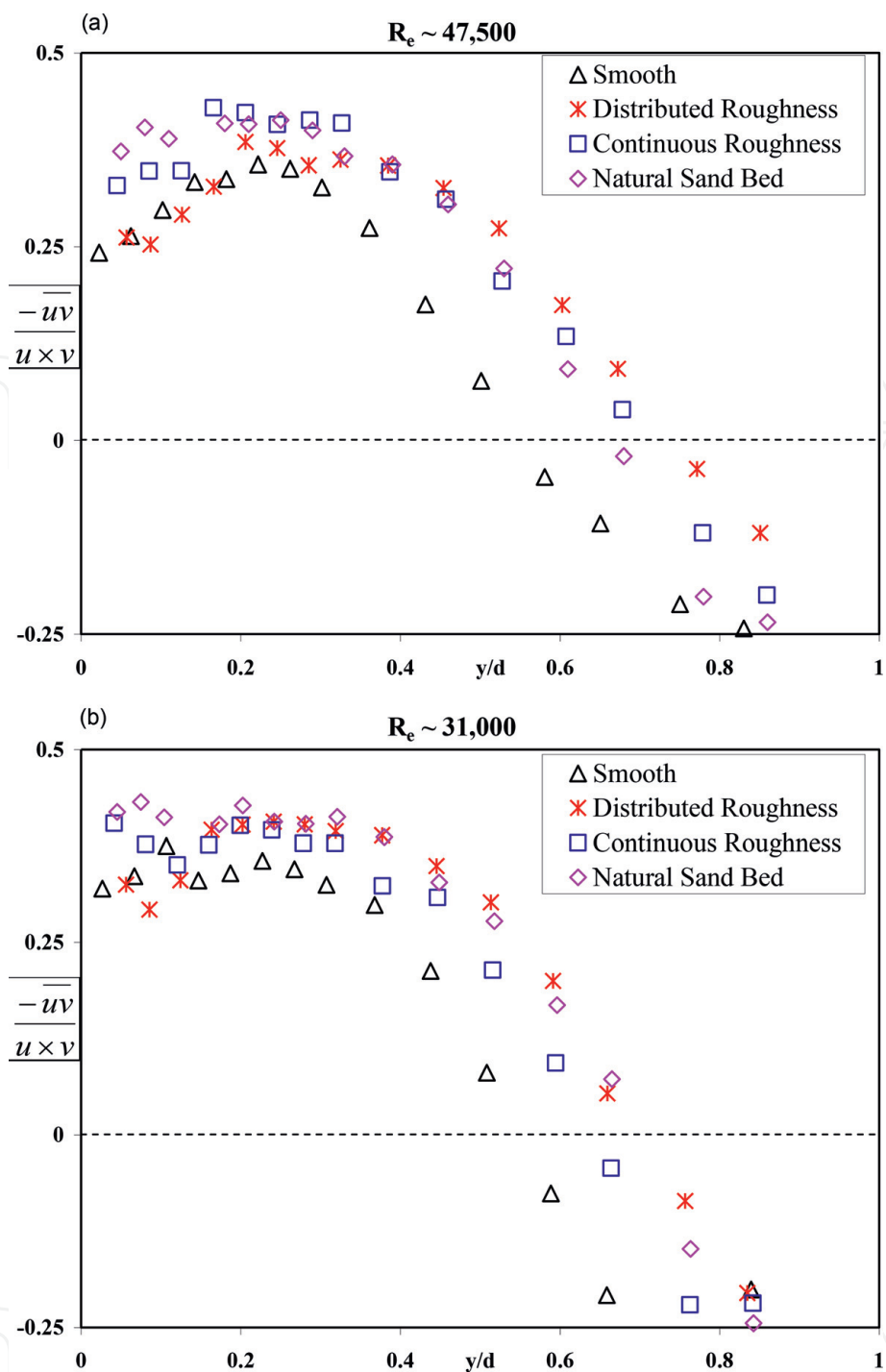


Figure 9.
Distribution of correlation coefficient for flow over different bed condition.

of R increases with the increasing distance from the bed and the trend reverses for the outer layer ($y > 0.3d$), indicating the changes of flow structure characteristics between the near-bed region and outer region. This observation is clearly different than the characteristics of R noted by [7, 5–6] where [7] called the distribution of R universal as they did not find any effect of roughness on the value of R . In Ref. [7] noted an existence of equilibrium region for $0.1 \leq y/d \leq 0.6$ with a value of $R = 0.4\text{--}0.5$ in open-channels, pipes, and boundary layers, irrespective of whether the wall bed is smooth or rough. In the inner region and for the flow over smooth bed, [6] found a much lower value of R and noted indifference of R value for the flow over rough and smooth bed for $y > 0.15d$ with the peak values floating to 0.35 ± 0.02 range. Comparing the effect of various type of bed roughness on the correlation coefficient as one can see from **Figure 9a** that distributed roughness has

the higher absolute value of R followed by continuous roughness and natural sand bed for the upper third of the flow. One can also note from **Figure 9a** that the value of R changes sign and become negative for flow over both smooth and rough bed surfaces at the locations where the Reynolds shear stress and dU/dy is negative. In the reference [6] also report similar observation. The value of R for the present study ranges from $-0.25 < R < 0.5$ and can be considered as small to medium correlation between the streamwise component and the vertical component of the turbulence intensity for all bed conditions and full depth of flow. The variation of the correlation coefficient of the Reynolds shear stress for flow over various bed surfaces with respect to the lower Reynolds number is shown in **Figure 9b**. The profile characteristics are very similar for the lower Reynolds number flow compared to the flow for higher Reynolds number with the exception that the profiles are more or less flatter for all bed conditions and bottom third of the flow. Another difference is that for the outer layer ($y > 0.3d$) flow the magnitude of R is higher for flow over natural sand bed compared to the flow over continuous roughness.

3.5 Higher-order moments

Velocity triple products $\overline{u^3}$, $\overline{u^2v}$, $\overline{v^3}$ and $\overline{v^2u}$ are very useful tools used by the researchers to extract valuable information of the flow structures and the distribution of different normalized velocity triple products are shown in **Figure 10**. To avoid any additional uncertainties by using computed quantities in relation to the scaling parameters, directly measured parameters of the maximum velocity (U_e) and the maximum flow depth (d) are used for normalizing all four velocity triple products. Streamwise flux of the turbulent kinetic energy u^2 and v^2 is defined by $\overline{u^3}$ and $\overline{v^2u}$ respectively whereas vertical transport/diffusion of the turbulent kinetic energy u^2 and v^2 is defined by $\overline{u^2v}$ and $\overline{v^3}$ respectively. Transportation in the direction normal to the bed for the Reynolds shear stress is also defined by $\overline{v^2u}$. Ejection-sweep cycle is considered to be the main turbulent motion contributing to the turbulent transport and velocity triple products are the tools used by the researchers to explain the ejection-sweep events effectively. Various bed conditions affect the variation of the different velocity triple products eventually provide insight about causing turbulent transport mechanisms change/modification.

For the flow condition over the smooth bed and very close to the bed, the magnitude of $\overline{u^3}$ is negative and $\overline{u^2v}$ is positive as one can note from **Figure 10a** and **b** indicating a fluid parcel slowly moving upward causing transportation of u momentum away from the bed representing an motion of ejection type. For the flow condition over the rough beds and very close to the bed, the magnitude of $\overline{u^3}$ is positive with very high comparable value and $\overline{u^2v}$ is negative as one can note from **Figure 10a** and **b** indicating a fast moving fluid parcel acting downwards causing transportation of u momentum towards the bed representing an motion of sweep type. Both triple products parameters of $\overline{u^3}$ and $\overline{u^2v}$ changes sign as one moves away from bed towards the free surface rendered changes of ejection-sweep cycle. The change of ejection-sweep cycle as one moving away from the bed is also observed by [27] and they had related this characteristic to the accompanying streaks of low-speed produced by the rough bed conditions and modification of the longitudinal vortices. The magnitude of $\overline{u^3}$ becomes more negative as one moves further away from the bed ($y/d > 0.08$) causing the sweeping events reduced substantially with the value of $\overline{u^3}$ fluctuates but stays negative for the depth throughout. The effect of roughness is also very evident for the value of $\overline{u^3}$ when compared with flow over smooth bed. The above mentioned differences between the flow over smooth bed

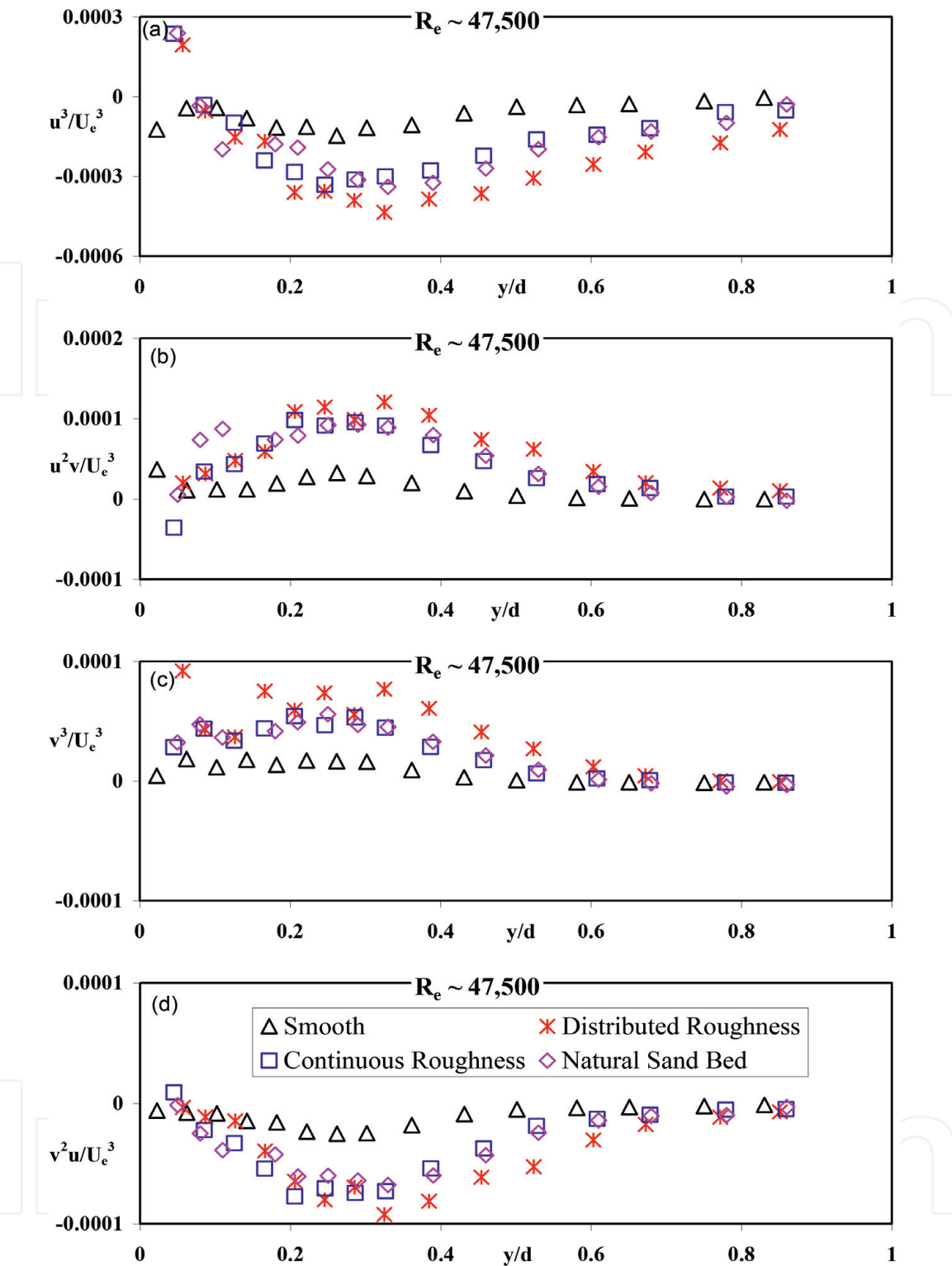


Figure 10.
Distribution of different velocity triple products for flow over different bed condition at $Re \sim 47,500$.

and rough beds are in complete opposite to the observation of [27–28] who did not observe much variation at distance $y/d > 0.2$. For flows over transverse rod roughness, large differences in the variation of $\overline{u^3}$ were observed by [29] upto to the edge of the boundary layer. This difference as related by [3] is related to the lack of formation of long streamwise vortices near the rough wall. Comparing flow over rough bed conditions with flow over smooth bed, the mechanics of the entrainment of low momentum fluid at the wall differed as noted by [3]. The variation trend for of $\overline{v^3}$ (Figure 10c) and $\overline{u^2v}$ (Figure 10b) are very similar but there are exception in

sign that throughout the depth the $\overline{v^3}$ is positive and much smaller magnitude ($\sim 60\%$) than $\overline{u^2v}$. The trend is qualitatively similar if one compare $\overline{v^2u}$ (**Figure 10d**) with $\overline{u^3}$ (**Figure 10a**) with the exception that the magnitude of $\overline{v^3}$ is about 60% less than that of $\overline{u^2v}$ but the magnitude of $\overline{v^2u}$ is much lower (about 20–25%) comparing magnitude of $\overline{u^3}$. In Refs. [6, 8] in their open channel flow experiments and [27–28] in their turbulent boundary layer experiments had also noted a similar reduction. The lower turbulent intensity in vertical direction is mainly the reason for the differences between $\overline{v^3}$ and $\overline{u^2v}$ and $\overline{v^2u}$ and $\overline{u^3}$. Comparing the magnitude of different velocity triple products for the open channel flow with the turbulent boundary layer flow, one can see the similarity as well as differences for magnitude and extent of the depth of the flow affected mainly in the outer layer by the roughness. As one can see from the **Figure 10** that the local peak (maxima/minima) for all normalized velocity triple products are in very similar location for the flow over smooth wall ($\approx 0.26d$). But the location of the peak (maxima/minima) for all normalized velocity triple products does not vary much with different type of roughness and occurs at a location of $y/d \approx 0.33$ for different rough beds. The magnitude of various velocity triple products changes in the range of 200–300% as one can note it from **Figure 10** when comparing the flow over the smooth bed to the flow over rough beds. The similar significant decrease/increase of the magnitude of various velocity triple products in the range of $\sim 300\%$ was also noticed by [8] when comparing the flow over the smooth bed to the flow over dunes. With the exception of the magnitude of $\overline{u^3}$ for the flow over distributed roughness, the magnitudes of the various velocity triple products approach zero for all smooth and rough surfaces as one moves from the location where the local maximum/minimum level achieved towards the free surface at $y/d > 0.85$.

The magnitude of various velocity triple product reaches near-zero at the location very close to the free surface irrespective of the bed surface conditions as one can note from **Figure 10** which is a clear indication of significant reduction of turbulent activity at near free surface. There is another significant finding one can note from the same figure that the type of bed roughness does not affect the location of maximum/minimum of various velocity triple product although there is clear effect of roughness on the magnitude of various velocity triple products. Flow over distributed roughness shows higher magnitude of various velocity triple product comparing with flow over other rough beds followed by very similar magnitude for flow over continuous roughness and natural sand bed. Turbulent activity at the near bed ($y/d < 0.1$) location also seen to be dependent on bed surface conditions. Flow over smooth bed shows the ejection type activity near bed location whereas the flow over rough beds show the sweep type activity at the location close to the bed. Interpolating this scenario to the real life stream or river flow, one can clearly note the influence of strong ejection/sweeping motion of the fluid parcels to the resuspension/transport of the bed particles. Ejection type events are very evident throughout the depth of flow with the exception of the location very close to the bed with flow over smooth bed only where one can observe some sweeping type of event. Bed surface conditions clearly affect the strength of the ejection like events with distributed roughness again shows the highest strength compared to similar strength from continuous bed roughness and natural sand bed. **Figure 11** shows the variation of same velocity triple products for the flow with respect to lower Reynolds number. The profile characteristics of all velocity triple products are very similar for flow with respect to lower Reynolds number compared to the flow with respect to higher Reynolds number. The differences in magnitude of various velocity triple products are seen to be reduced in the case of lower Reynolds number flow comparing the flow over smooth bed to the flow over continuous bed roughness and

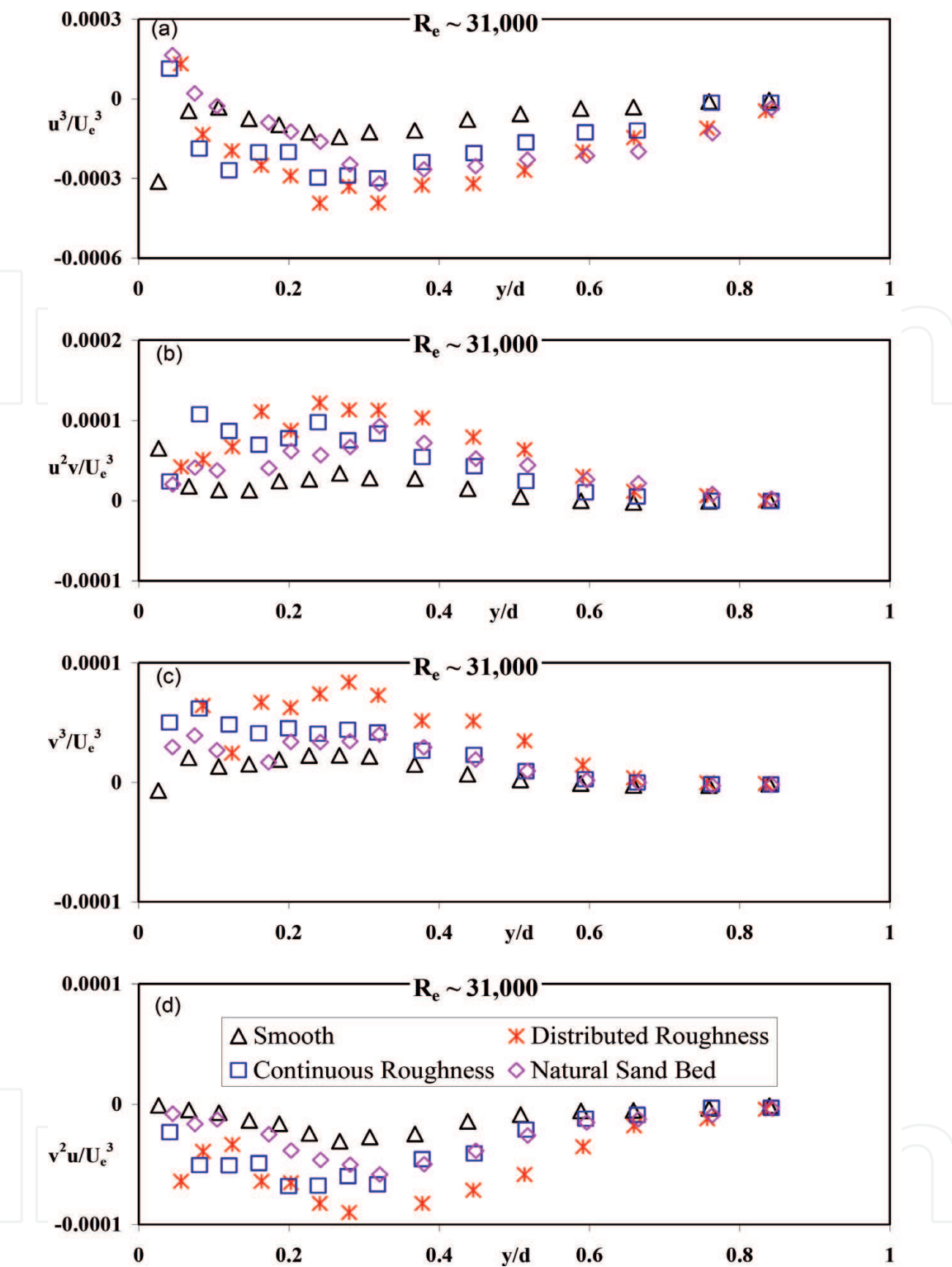


Figure 11.
Distribution of different velocity triple products for flow over different bed condition at $R_e \sim 31,000$.

natural sand bed. The value of $\overline{u^3}$ is also reaches near-zero close to the free surfaces irrespective of the bed conditions representing a vanishing turbulent activity at that location.

3.6 Vertical flux of the turbulent kinetic energy

The distribution of the vertical flux of the turbulent kinetic energy described as F_{kv} and which is normally measured as $0.5(\overline{v^3} + \overline{vu^2})$ for a two-dimensional flow [8]

is shown in **Figure 12** in outer variables for the flow over both smooth and rough beds. The LDA used to measure the velocity component is two-dimensional and not possible to measure the third component of turbulent intensity. An approximate method as proposed by [30] is used to overcome this shortcoming and the coefficient is changed from 0.75 to 0.5. The effect of roughness is very evident for the transport of the turbulent kinetic energy in the vertical direction as one can see from **Figure 12**. The effect of roughness is not only confined for near bed but can be seen throughout the depth of flow. This observation is in direct conflict with the observation of [8] who in their tests with large-bottomed roughness did not visualize notable differences in profile for the vertical flux of the turbulent kinetic energy when comparing open channel flow over smooth bed and rough bed conditions.

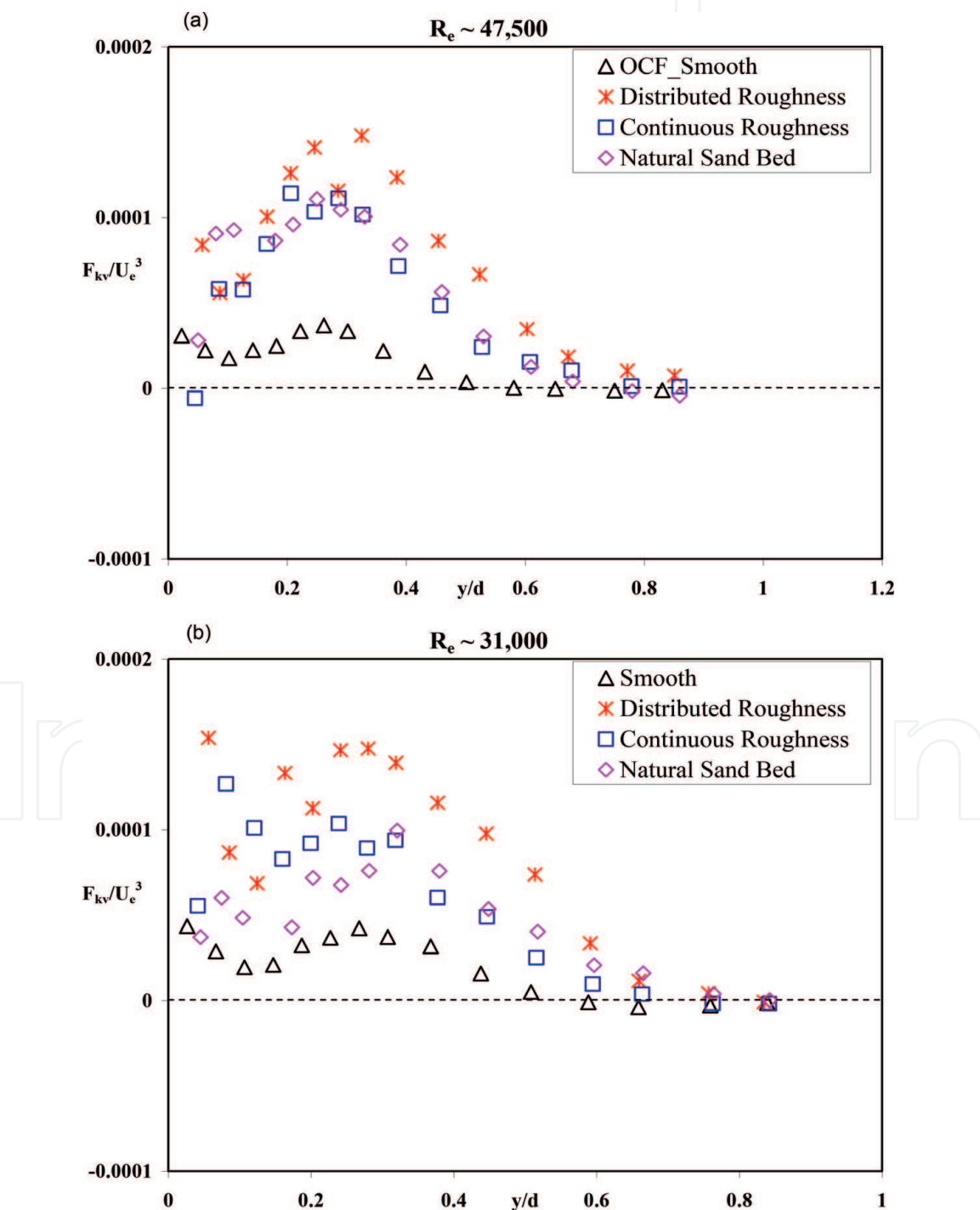


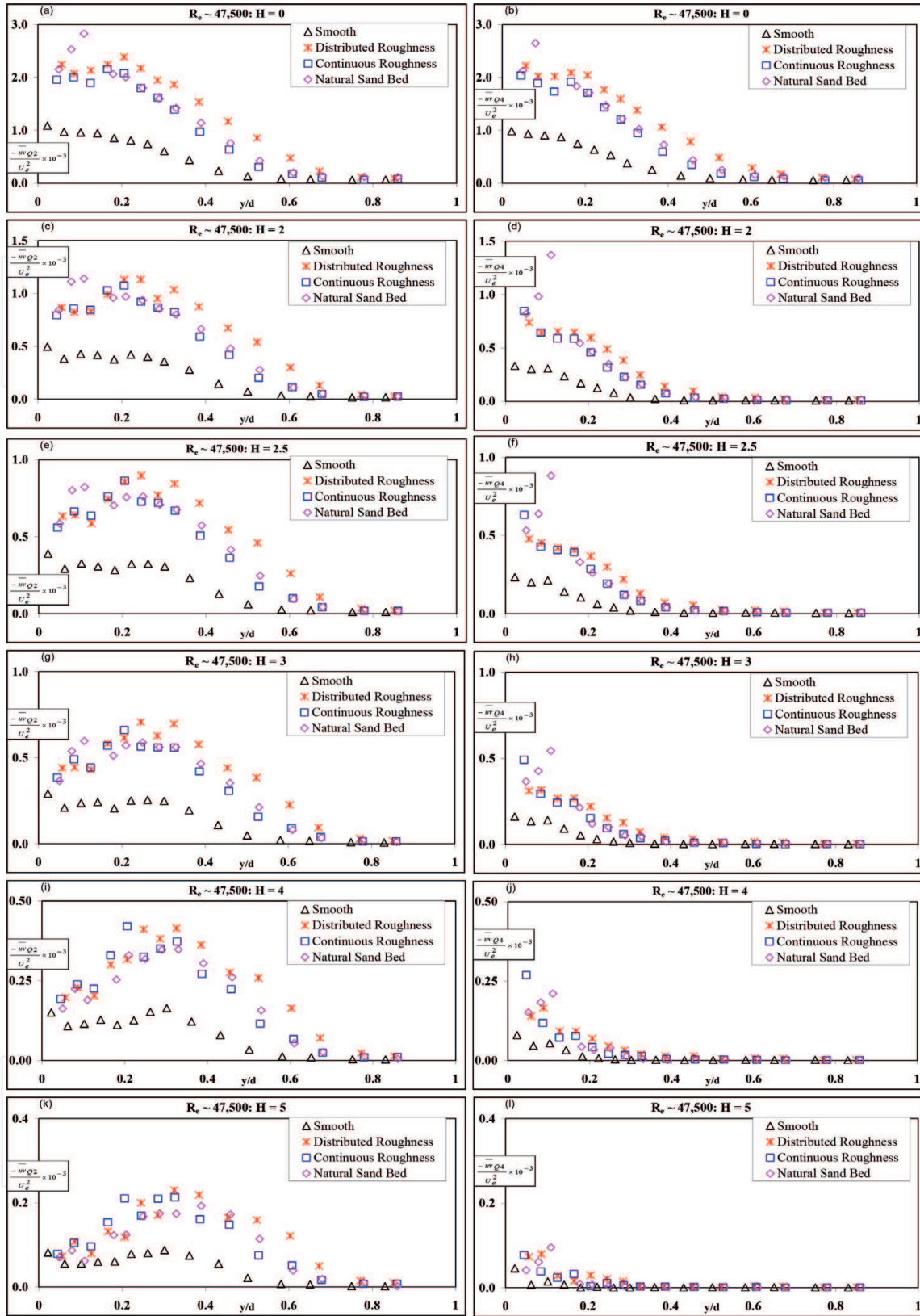
Figure 12.
Distribution of vertical flux of the turbulent kinetic energy for flow over different bed condition.

In Ref. [6] noted that the location of the outer (larger) peak of F_{kv} is closer to the wall (albeit slightly) as the roughness effect increases. The maximum value of F_{kv} is also noted in Ref. [8] where they found it occurred near the bed for the flow over rib roughness. As one can note from **Figure 12** that there are obvious effect of roughness on the variation of the vertical flux of the turbulent kinetic energy with the magnitude of the peak is very different for different type of rough surfaces but the location of the peak for all rough beds are more or less at around $y/d \sim 0.3$. The differences in magnitude of the vertical flux of the turbulent kinetic energy when comparing between smooth bed flow and flow over rough beds is a clear indication that the strength of the vertical flux of the turbulent kinetic energy is very different for flow over different surfaces. The slope of the variation of F_{kv} is different between smooth and rough beds representing difference in loss or gain of turbulent kinetic energy resulted from turbulent diffusion. Flow over distributed roughness shows the highest deviation compared to the flow over smooth bed. The vertical flux of the turbulent kinetic energy approaches near zero value after a peak value around $y/d = 1$ at the location near free surface for all bed conditions. Location of reaching zero value for the vertical flux of the turbulent kinetic energy also varies with the bed surface condition with flow over different rough beds show zero values closer to the free surface compared to the flow over smooth bed. **Figure 12b** shows the variation of the vertical flux of the turbulent kinetic energy for the flow with respect to lower Reynolds number. The profile characteristics are very similar for flow with respect to lower Reynolds number compared to the flow with respect to higher Reynolds number. The differences in magnitude of F_{kv} is seen to be reduced in the case of lower Reynolds number flow comparing the flow over smooth bed to the flow over continuous bed roughness and natural sand bed.

3.7 Quadrant analysis

In order to extract the magnitude of the Reynolds shear stress related to turbulent bursting events researchers often use quadrant decomposition as a convenient tool. A hydro dynamically unstable low-speed fluid particle lifted up from the surface because of the turbulent flow over a fixed bed can be swept away by comparatively high-speed fluid from the outer layer moving towards the bed surface. All different type of turbulent flow events that eventually contributed in the four different very important turbulent characteristics closer to the wall can be described by coupling streamwise and vertical fluctuating velocity components u and v based on their sign. Four different quadrants formed by using u and v with proper sign are related to four very important turbulent bursting events. Quadrant 1 represents the bursting effect called as outward interaction where the value of u is >0 and the value of v is >0 . Quadrant 2 represents the bursting effect called as ejection where the value of u is <0 and the value of v is >0 . Quadrant 3 represents the bursting effect called as inward interaction where the value of u is <0 and the value of v is <0 . Quadrant 4 represents the bursting effect called as sweep where the value of u is >0 and the value of v is <0 .

The contributions from Q2 and Q4 events for different threshold values to the Reynolds shear stress are shown in **Figure 13** with higher Reynolds number ($Re = 47,500$). For the flow over rough walls and inclusive of all turbulent events, it was noted higher magnitude of Q2 and Q4 contributions as shown in **Figure 13a** and **b** compared to the flow over smooth wall for $H = 0$. The effect of roughness is not limited to the near-bed region but well progressed into the outer layer ($y/d \approx 0.7$). A local peak can be seen at $y/d = 0.1-0.2$ for the Q2 and Q4 contributions as one progresses from the bed towards the free surface for the flow over all rough beds. The peak magnitudes of both of the events eventually reduced

**Figure 13.**

Contribution of different quadrant events to the Reynolds shear stress for flow over different bed condition with higher Reynolds number.

to a near-zero constant value as flow moves towards the free surface. The location where the contributions from Q2 and Q4 events attains a near-zero constant value is not the same but varied with bed conditions. For the smooth bed condition the distance of the attainment of near-zero constant value is $0.5d$ from the bed, for the continuous roughness and sand bed condition the distance is $0.6d$ from the bed and for the distributed roughness the distance is $0.75d$ from the bed. Different rough

bed conditions show different deviation from smooth wall with distributed roughness showing the highest deviation. The maximum deviation comparing the flow over smooth wall with the flow over rough bed occurs at a depth of around $0.2d$ from the bed with distributed roughness shows the highest deviation and continuous roughness and sand bed show almost equal deviation. In Ref. [31] found significantly higher magnitude of Q2 and Q4 events in the region very close to the bed but found very similar distribution for the flow over smooth bed and rough beds for the outer layer.

In order to investigate the contribution of the extreme turbulent events quadrant analysis at different threshold levels ($H = 2-5$) was also carried out. The respective approach was taken to take care of the contribution of the more energetic eddies and filtering out the small random turbulent fluctuations. The contributions from the extreme events whose amplitude exceeds the threshold value of $H = 2$ are shown in **Figure 13c** and **d**. Although due to the change of threshold value from 0 to 2, the number of events occurring corresponding to Q2 and Q4 reduce quite sharply but the events corresponding to $H = 2$ produced very large instantaneous Reynolds shear stress ($>5.5 \overline{uv}$), which can potentially influence the sediment transport in the stream, causing resuspension of pollutant from the bed, bed formation/changes, downstream transportation of nutrients, entrainment and the exchange of energy and momentum in the flow. The trend of the data at $H = 2$ is very close to $H = 0$, however, the region of the flow depth affected for Q4 events reduces compared to $H = 0$. The contributions related to other threshold levels of $H = 2.5-5$ are shown in **Figure 13e-i** and one can observe that the region affected over the depth of flow for Q4 events reduces with respect to the increase of the threshold level of H but the affected region goes deep into the outer layer ($y \sim 0.7d$) for the Q2 events even for the value of H as high as 5. The incorporation of roughness is clearly visible in the increase in both Q2 and Q4 contribution to the Reynolds shear stress, irrespective of the affected region of the depth. Much stronger Q2 events were observed by [31–32] on a flow over a smooth wall when compared to the flow over a rough wall for the location close to the bed and they relate the phenomena for the smooth wall to the contributions of strongly favored Reynolds stress from ejection (Q2 events). The differences in observation between the turbulent boundary layer flow and open channel flow can confirm that turbulent bursting and eventual production of Reynolds shear stress due to ejection (Q2 events) and sweep (Q4 events) is different for the flow in open channel. Significant ejection and sweep components were noted by [8] with ejection events being dominant throughout the depth of flow and they also noted that different types of rib roughness result significant variations. One can notice in the present study that Q2 and Q4 events are dependent on the bed roughness accompanied by significant drop near the free surface for both events, signifies the important role the bed roughness type possesses on Q2 and Q4 events. At the location near bed, generation of turbulent activity varies with the type of bed roughness. Low momentum slow moving fluid from the near-bed is ejected and travels towards the outer layer/free surface and the same will happen for the fluid between the interstices of the roughness. In contrast, high momentum fast moving fluid from the outer layer travels towards bed, sweeping away the low momentum slow moving fluid parcels ejected earlier. The extent of depth of flow affected by the existence of universal intermittent sweep and ejection events is dependent on the type of bed and the flow condition. **Figure 14** shows the variation of the contributions from Q2 and Q4 events for different threshold values to the Reynolds shear stress with lower Reynolds number ($Re = 31,000$). The profile characteristics are very similar for flow with respect to lower Reynolds number compared to the flow with respect to higher Reynolds number for the threshold values of $H = 0-5$.

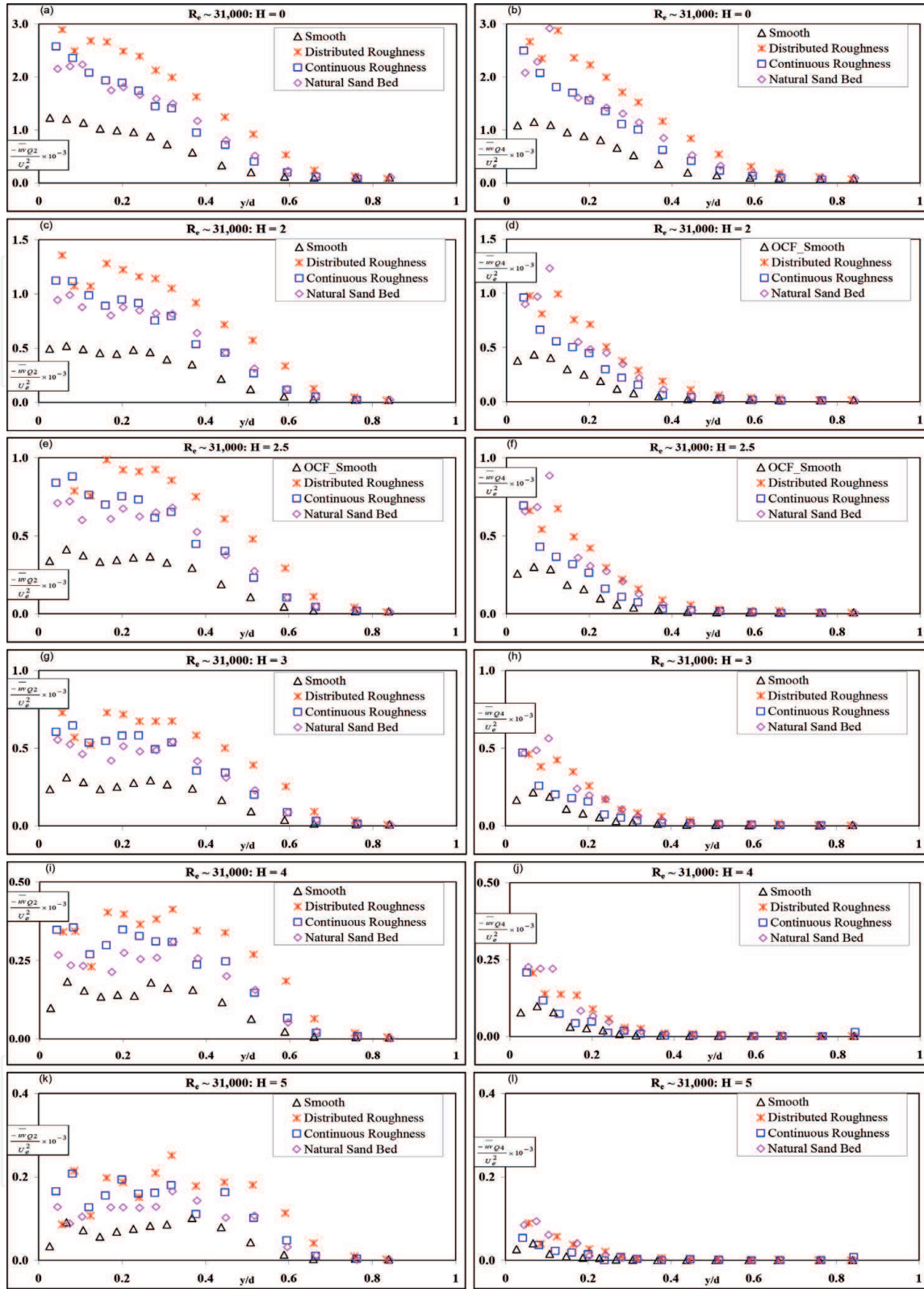


Figure 14.

Contribution of different quadrant events to the Reynolds shear stress for flow over different bed condition with lower Reynolds number.

Figure 15 shows the ratio to the Reynolds shear stress contributions of Q2/Q4 for $H = 0-5$ and for two different Reynolds numbers. The Q2/Q4 ratio is near unity at the location very close to the bed indicating identical strength of sweep and ejection event as one can note from Figure 15. The Q2/Q4 ratio increases from near unity to maximum at around mid-depth of the flow ($y/d \sim 0.5$) as one progress from the bed and towards the free surface which is an indication of relatively stronger

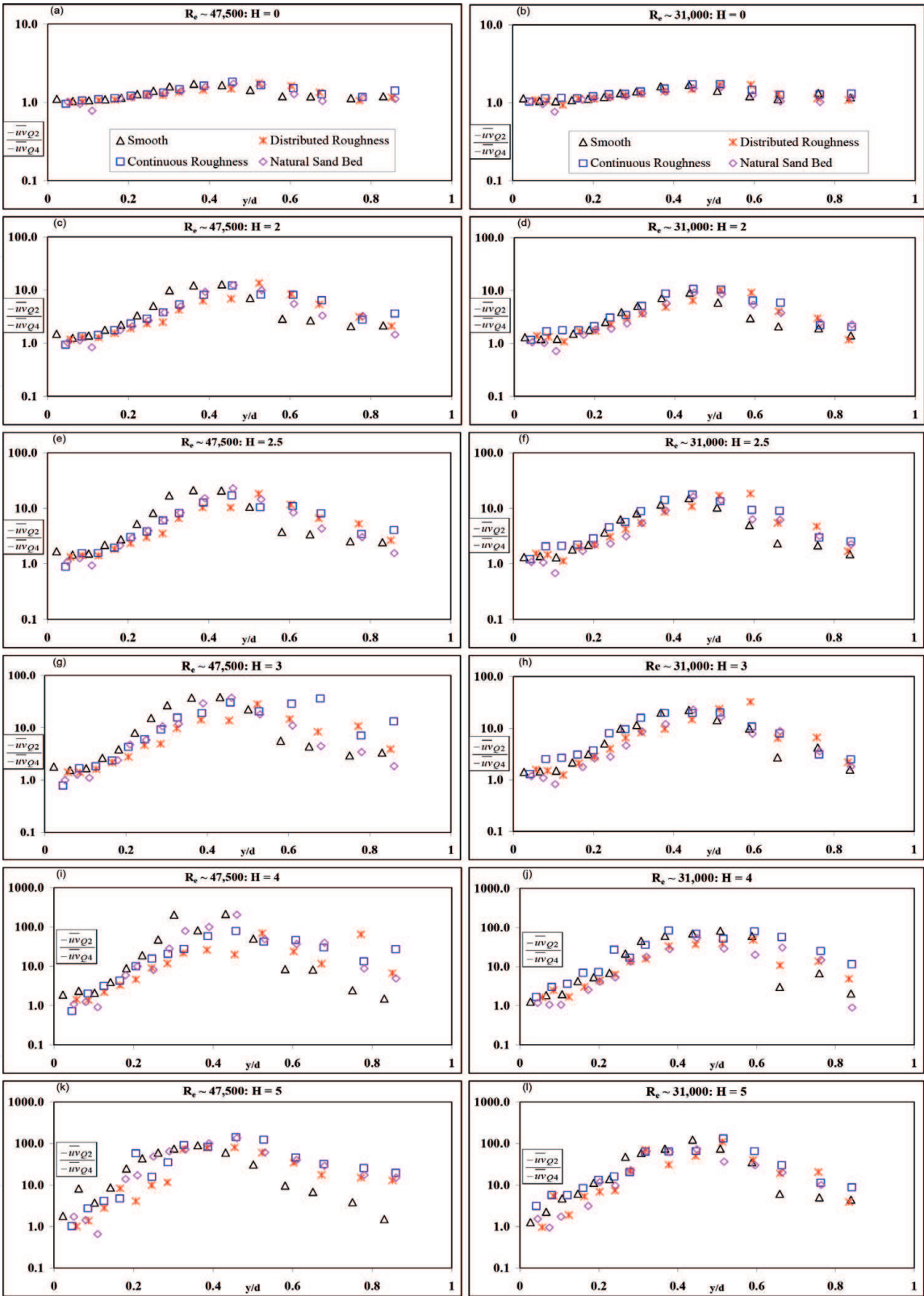


Figure 15.
Ratio of different quadrant events to the Reynolds shear stress for flow over different bed condition.

ejection events compared to the sweep events. The corresponding strength of the ejection events increases in comparison to sweep events with respect to increasing H and as one can note from the **Figure 15** that there is a 100 over fold increase for the threshold value of $H = 5$ compared to $H = 0$. As one can also note from **Figure 15** that there is little dependency on bed conditions of smooth and rough for $H = 0$ on the ratio of Reynolds shear stress in Q2 and Q4 but for the same value of $H = 0$ there are some effect of roughness for $y > 0.5d$.

Figure 16 shows the ratio to the number of events occurring/contributing in Q2 and Q4 for $H = 0-3$ and for two different Reynolds numbers. The ratio to the number of events occurring/contributing to Q2 and Q4 shows different trends for the threshold value of $H = 0$ (**Figure 16a** and **b**) compared to the threshold value of $H = 2-3$ (**Figure 16c-h**). This is very unlike to the ratio of the Reynolds shear stress contributions of Q2/Q4 as shown in **Figure 15**. The N_{Q2}/N_{Q4} ratio is near unity at the location very close to the bed indicating almost equal occurrence of ejection and sweep events as one can note from **Figure 16a** and **b**. The N_{Q2}/N_{Q4} ratio decreases from near unity to minimum at around mid-depth of the flow ($y/d \sim 0.5$) as one progress from the bed and towards the free surface which is an indication of relatively reduced ejection events compared to the sweep events. Moving farther away from bed ($y > 0.5d$) and towards the free surface, the ratio of N_{Q2}/N_{Q4} ratio is keep on increasing again and reaches to near unity indicating almost equal occurrence of ejection and sweep events. **Figure 16c-h** show a trend different from **Figure 16a** and **b**. As one progress from the bed towards the free surface, there is an increment of 30 over fold for the value of N_{Q2}/N_{Q4} at around $y \sim 0.5d$, indicating substantial increase of ejection events. As one can also note from **Figure 16** that there is little dependency on bed conditions of smooth and rough for $H = 0$ on the ratio of number of events in Q2 and Q4.

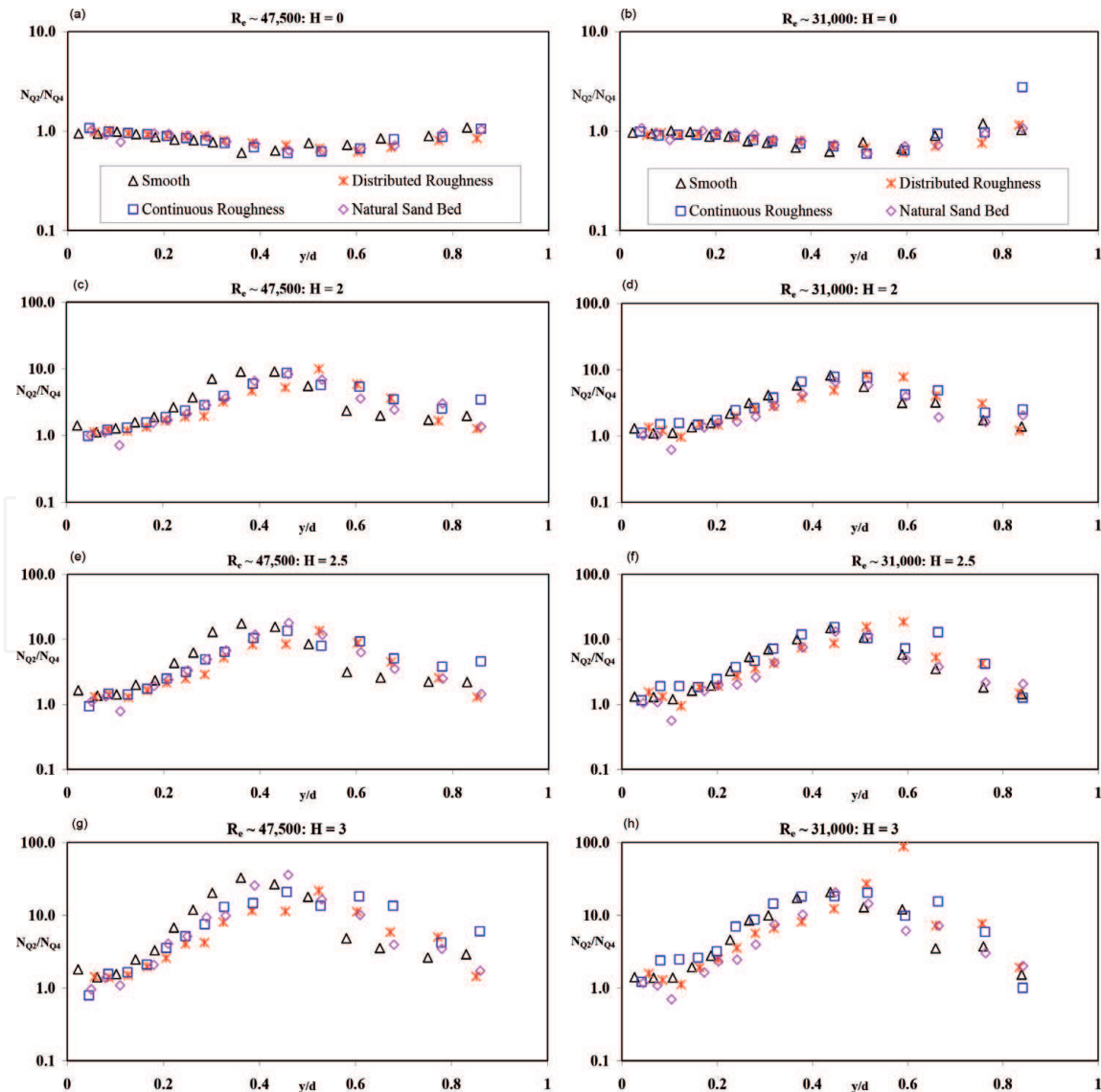


Figure 16.
Ratio of number of different quadrant events for flow over different bed condition.

4. Conclusions

The purpose of the present study [1] is to explain how the roughness and Reynolds number affect flow characteristics in an open channel flow (OCF). Tests were conducted with four different types of bed surface conditions and at two different Reynolds number for each and every bed surface. Instantaneous velocity components are used to analyze the streamwise mean velocity, turbulence intensity in both streamwise and vertical direction, Reynolds shear stress including shear stress correlation and higher-order moments including vertical flux of the turbulent kinetic energy. In order to extract the magnitude of the Reynolds shear stress related to turbulent bursting events quadrant decomposition was used. The main findings are summarized as follows:

1. Surface drag increases due to surface roughness making the mean streamwise velocity profile to be more fuller for the smooth bed compared to the rough beds. It is very much evident throughout the depth of the flow that the mean velocity profile is very much affected by the different type of bed roughness. Comparing the effect of various type of bed roughness on the streamwise velocity component and flow with higher flow Reynolds number, distributed roughness profile has the biggest deviation from smooth bed profile with continuous roughness and natural sand bed shows identical deviation. For the flow with lower flow Reynolds number, it was found that the flow over natural sand bed shows much higher deviation than flow over the bed of continuous roughness.
2. The magnitude of friction coefficient is found to be dependent on the type of bed roughness with distributed roughness has the highest value followed by the flow over the continuous roughness bed surface and the sand bed. The magnitude of friction coefficient is also found to be dependent on the Reynolds number with the reduction of the magnitude of friction coefficient with the increment of the Reynolds number. The magnitude of friction coefficient is seen to be smaller for the flow over a permeable bed (natural sand bed) compared to the flow over an impermeable bed (distributed and continuous roughness bed).
3. The effect of roughness on the distribution of the streamwise component of the turbulence intensity is very evident throughout the flow depth with distributed roughness shows the highest deviation followed by natural sand bed and continuous roughness compared to the smooth surfaces with the exception at the location very close to the bed. Comparing the effect of various type of bed conditions on the vertical component of the turbulence intensity, it was seen that distributed roughness profile has the biggest deviation from smooth bed profile with continuous roughness and natural sand bed shows identical deviation for most the depth of the flow. At locations very close to the bed and due to the introduction of roughness, streamwise turbulence intensity reduces but vertical turbulence intensity increases. Although the sand grain used to create all three bed roughness is of the same gradation characteristics but the specific geometry of the roughness formation is different causing the differences in the formation of turbulence structure.
4. Wall similarity hypothesis is disputed by the present experimental results where the researchers suggested that in the location of outside the roughness

layer, the turbulent mixing properties should be essentially the same for the flow over smooth and rough walls which was initially proposed by [33] and generalized by [34].

5. Effect of roughness on the Reynolds shear stress is very evident at the location close to the bed generating much higher Reynolds shear stress than the smooth bed. The distinct effect of roughness for the present study can be seen penetrating deep into the flow and distinctly visible at the location as high as $y/d \approx 0.7$.
6. The trend of the changes of the value of R (correlation coefficient) in the near-bed and outer layer indicating the changes of flow structure characteristics between the near-bed region and outer region. The present results clearly dispute the observation of [5] that the distribution of R is independent of the properties of the wall roughness, mean flow, and called the distribution of R is universal.
7. The magnitude of various velocity triple products changes in the range of 200–300% when comparing the flow over the smooth bed to the flow over rough beds. This is a clear indication that the transportation of turbulent kinetic energy and Reynolds shear stress is significantly affected by the bed roughness.
8. Turbulent activity at the near bed location also seen to be dependent on bed surface conditions. Flow over smooth bed shows the ejection type activity near bed location whereas the flow over rough beds show the sweep type activity at the location close to the bed. Interpolating this scenario to the real life stream or river flow, one can clearly note the influence of strong ejection/sweeping motion of the fluid parcels to the resuspension/transport of the bed particles.
9. Ejection type events are very evident throughout the depth of flow with the exception of the location very close to the bed with flow over smooth bed only where one can observe some sweeping type of event. Bed surface conditions clearly affect the strength of the ejection like events with distributed roughness again shows the highest strength compared to other form of bed roughness.
10. Effect of roughness is clearly visible well beyond the near-bed region and deep into the outer layer ($y \approx 0.7d$) from the analysis/result of turbulent bursting events (through quadrant decomposition). For the flow over rough walls and inclusive of all turbulent events, it was noted higher magnitude of $Q2$ and $Q4$ contributions compared to the flow over smooth wall for $H = 0$.
11. Analysis were also carried out to investigate the contribution of the extreme turbulent events at different threshold levels ($H = 2-5$). The region affected over the depth of flow for active sweep ($Q4$) events reduces with respect to the increase of the threshold level of H but the affected region goes deep into the outer layer ($y \sim 0.7d$) for the active ejection ($Q2$) events even for the value of H as high as 5. Although due to the change of threshold value from 0 to 2, the number of events occurring corresponding to $Q2$ and $Q4$ reduce quite sharply but the events corresponding to $H = 2$ produced very large instantaneous Reynolds shear stress ($>5.5 \bar{u}\bar{v}$), which can potentially influence the sediment transport in the stream, causing resuspension of pollutant from the bed, bed formation/changes, downstream transportation of nutrients, entrainment and the exchange of energy and momentum in the flow.

12. The ratio to the Reynolds shear stress contributions of Q2/Q4 is near unity at the location very close to the bed and location close to the free surface indicating identical strength of sweep and ejection. With the exception of near bed and near free surface, relatively stronger ejection events compared to the sweep events can be seen for throughout the flow depth and the strength of the ejection events increases many fold with increase of the threshold value of H .
13. The ratio to the number of events occurring/contributing in Q2 and Q4 is near unity at the location very close to the bed and location close to the free surface indicating almost equal occurrence of sweep and ejection events. With the exception of near bed and near free surface, relatively reduced ejection events compared to the sweep events can be seen for throughout the flow depth for $H = 0$ but shows substantial increase of ejection events compared to the sweep events for $H > 0$.


IntechOpen

Author details

Abdullah Faruque
Civil Engineering Technology, Rochester Institute of Technology, Rochester,
New York, USA

*Address all correspondence to: aafite@rit.edu

IntechOpen

© 2019 The Author(s). Licensee IntechOpen. This chapter is distributed under the terms of the Creative Commons Attribution License (<http://creativecommons.org/licenses/by/3.0>), which permits unrestricted use, distribution, and reproduction in any medium, provided the original work is properly cited. 

References

- [1] Faruque MAA. Smooth and rough wall open channel flow including effects of seepage and ice cover [PhD thesis]. Windsor, Canada: University of Windsor; 2009
- [2] Rashidi M, Hetsroni G, Banerjee S. Particle-turbulence interaction in a boundary layer. *International Journal of Multiphase Flow*. 1990;**16**(6):935-949
- [3] Grass AJ. Structural features of turbulent flow over smooth and rough boundaries. *Journal of Fluid Mechanics*. 1971;**50**(2):233-255
- [4] Nakagawa H, Nezu I. Prediction of the contributions to the Reynolds stress from bursting events in open-channel flows. *Journal of Fluid Mechanics*. 1977; **80**(1):99-128
- [5] Nezu I, Nakagawa H. Turbulence in open-channel flows. IAHR Monograph. In: Balkema AA, editor. Rotterdam, Netherlands; 1993
- [6] Tachie MF. Open-channel turbulent boundary layers and wall jets on rough surfaces [PhD thesis]. Saskatchewan, Canada: University of Saskatchewan; 2001
- [7] Nezu I. Open-channel flow turbulence and its research prospect in the 21st century. *Journal of Hydraulic Engineering*. 2005;**131**(4):229-246
- [8] Balachandar R, Bhuiyan F. Higher-order moments of velocity fluctuations in an open channel flow with large bottom roughness. *Journal of Hydraulic Engineering*. 2007;**133**(1):77-87
- [9] Afzal B, Faruque MAA, Balachandar R. Effect of Reynolds number, near-wall perturbation and turbulence on smooth open channel flows. *Journal of Hydraulic Research*. 2009;**47**(1):66-81
- [10] Patel VC. Perspective: Flow at high Reynolds number and over rough surfaces—Achilles heel of CFD. *Journal of Fluids Engineering*. 1998;**120**(3): 434-444
- [11] Roussinova V, Biswas N, Balachandar R. Revisiting turbulence in smooth uniform open channel flow. *Journal of Hydraulic Research*. 2008;**46** (Suppl. 1):36-48
- [12] Kirkgöz MS, Ardiçhoğlu M. Velocity profiles of developing and developed open channel flow. *Journal of Hydraulic Engineering*. 1997;**123**(2):1099-1105
- [13] Tachie MF, Bergstrom DJ, Balachandar R. Roughness effects in low- Re_θ open-channel turbulent boundary layers. *Experiments in Fluids*. 2003;**35**:338-346
- [14] Balachandar R, Patel VC. Rough wall boundary layer on plates in open channels. *Journal of Hydraulic Engineering*. 2002;**128**(10):947-951
- [15] Tachie MF, Bergstrom DJ, Balachandar R. Rough wall turbulent boundary layers in shallow open channel flow. *Journal of Fluids Engineering*. 2000;**122**:533-541
- [16] Kaftori D, Hetsroni G, Banerjee S. Particle behavior in the turbulent boundary layer. I. Motion, deposition, and entrainment. *Physics of Fluids*. 1995;**7**(5):1095-1106
- [17] Dancey CL, Balakrishnan M, Diplas P, Papanicolaou AN. The spatial inhomogeneity of turbulence above a fully rough, packed bed in open channel flow. *Experiments in Fluids*. 2000; **29**(4):402-410
- [18] Tachie MF, Bergstrom DJ, Balachandar R. Roughness effects on the mixing properties in open channel

- turbulent boundary layers. *Journal of Fluids Engineering*. 2004;**126**:1025-1032
- [19] Bigillon F, Niño Y, Garcia MH. Measurements of turbulence characteristics in an open-channel flow over a transitionally-rough bed using particle image velocimetry. *Experiments in Fluids*. 2006;**41**(6):857-867
- [20] Faruque MAA, Sarathi P, Balachandar R. Clear water local scour by submerged three-dimensional wall jets: Effect of tailwater depth. *Journal of Hydraulic Engineering*. 2006;**132**(6): 575-580
- [21] Sarathi P, Faruque MAA, Balachandar R. Scour by submerged square wall jets at low densimetric Froude numbers. *Journal of Hydraulic Research*. 2008;**46**(2):158-175
- [22] Schlichting H. *Boundary-Layer Theory*. McGraw-Hill Classic Textbook Reissue Series. United States of America: McGraw-Hill, Inc; 1979
- [23] Bey A, Faruque MAA, Balachandar R. Two dimensional scour hole problem: Role of fluid structures. *Journal of Hydraulic Engineering*. 2007;**133**(4): 414-430
- [24] Zagni AFE, Smith KVH. Channel flow over permeable beds of graded spheres. *Journal of Hydraulics Division: Proceedings of the ASCE*. 1976;**102** (HY2):207-222
- [25] Krogstad P-A, Andersson HI, Bakken OM, Ashrafian A. An experimental and numerical study of channel flow with rough walls. *Journal of Fluid Mechanics*. 2005;**530**:327-352
- [26] Agelinchaab M, Tachie MF. Open channel turbulent flow over hemispherical ribs. *International Journal of Heat and Fluid Flow*. 2006;**27**(6): 1010-1027
- [27] Schultz MP, Flack KA. The rough-wall turbulent boundary layer from the hydraulically smooth to the fully rough regime. *Journal of Fluid Mechanics*. 2007;**580**:381-405
- [28] Flack KA, Schultz MP, Shapiro TA. Experimental support for Townsend's Reynolds number similarity hypothesis on rough walls. *Physics of Fluids*. 2005; **17**(3):35102-351-9
- [29] Antonia RA, Krogstad P-A. Turbulence structure in boundary layers over different types of surface roughness. *Fluid Dynamics Research*. 2001;**28**(2):139-157
- [30] Krogstad P-A, Antonia R. Surface roughness effects in turbulent boundary layers. *Experiments in Fluids*. 1999;**27**: 450-460
- [31] Schultz MP, Flack KA. Outer layer similarity in fully rough turbulent boundary layers. *Experiments in Fluids*. 2005;**38**:328-340
- [32] Krogstad P-A, Antonia R, Browne LWB. Comparison between rough and smooth-wall turbulent boundary layers. *Journal of Fluid Mechanics*. 1992;**245**: 599-617
- [33] Townsend AA. *The Structure of Turbulent Shear Flow*. Cambridge, United Kingdom: Cambridge University Press; 1976
- [34] Raupach MR, Antonia RA, Rajagopalan S. Rough wall turbulent boundary layers. *Applied Mechanics Review*. 1991;**44**(1):1-25